5-2014

Developing a cardiomyocyte proliferation probe utilizing non-degradable CKAP2.

Suraj Kannan
University of Louisville

Developing a Cardiomyocyte Proliferation Probe Utilizing Non-Degradable CKAP2

A dissertation presented

by

Suraj Kannan

to

The Department of Chemistry

in partial fulfillment of the requirements

for Graduation *summa cum laude*

for the degree of

Bachelor of Science

in the subject of

Chemistry with Concentration in Biochemistry

University of Louisville

Louisville, Kentucky

April 2014

Thesis advisor

Dr. Kyung Hong

Author

Suraj Kannan

Developing a Cardiomyocyte Proliferation Probe Utilizing Non-Degradable CKAP2

Abstract

Currently, one of the biggest controversies in the field of cardiac regenerative medicine revolves around the ability of cardiomyocytes to proliferate. In contrast to the long-held hypothesis that the heart is a terminally differentiated, post-mitotic organ, some studies have suggested that the heart is capable of undergoing limited regeneration following injury. Others have reported induction of cardiomyocyte proliferation following various treatments, mostly *in vitro*. Conventional tools such as BrdU labeling fail to distinguish between mitotic events and other phenomena such as endoreduplication or poly-nucleation, thus making it difficult to assess cardiomyocyte proliferation. The present study presents a novel and innovative way to unambiguously study cardiomyocyte proliferation by use of a cell division probe to identify cells that undergo mitosis. The system utilizes a mutant form of the mitotic regulator cytoskeleton-associated protein 2 (CKAP2). CKAP2 remains cytoplasmic during interphase, but translocates to the nucleus following mitotic cell division. Usually, wild-type CKAP2 is degraded via the ubiquitin-proteosome pathway following translocation to the nucleus; however, by mutation of a destruction motif, the protein persists in the daughter nuclei following cell division. Thus, this non-degradable mu-

tant of CKAP2 (ndCKAP2) can be used to track mitotic events - ndCKAP2 should remain cytoplasmic in quiescent cells but appear nuclear in cells that have undergone mitosis. Here, the efficacy of ndCKAP2 as a cell division probe is demonstrated; in particular, ndCKAP2 is demonstrated to be easily visualizable, unambiguously track mitotic events, and present a relatively long half-life (and is therefore integrative in output). It is expected that future studies will utilize this molecular probe system to investigate cardiomyocyte proliferation *in vivo* under a variety of physiological and pathological conditions, and allow for assessment of various proposed clinical therapies.

Acknowledgments

"Basic research is what I am doing
when I don't know what I am doing."
–Wernher von Braun

It is fair to say that when I first started working the lab about two and a half years ago, I had no idea what I was doing. Oh, sure, I understood what cell culture was, and how to run a gel, and could discuss the concept of a cell division probe. But the truth was, I had no idea how to do science. Working on a scientific research project is a daunting and consuming task, and my first days were spent coming to the realization that behind the cool and flashy exteriors of the scientific world lay a lot of unnerving challenges. These days, wherever we turn, we see amazing ideas being born out of brilliant minds - new studies, new technologies, new discoveries, and new science. But each of these successes was the result of a hard-won battle, fought by determined researchers who on a daily basis had to confront systems that simply wouldn't respond to their entreaties for knowledge. Even the best of scientists sometimes struggle to make those piercing insights that characterize the profession, so needless to say, I was rather out of my depth when I began this project. High school science courses had taught me the words "control and "hypothesis, but never before had I really thought hard about the concepts of experimental design. If you told me to look into the literature, I would have more likely ended up going to Hemingway than to *Nature*, so little did I know about the need to access primary research. Worst of all, I had no idea what to do when things didn't work the way I expected them to. All in all, it's something of a miracle that I accomplished anything at all!

However, these last several years and all the hours spent in the lab have served

as a magnificent learning experience, a chance to get started on what I hope will be a long and productive path into the world of science. I have been aided at each step by a number of friends, colleagues, and mentors, who have guided me along as I have slowly worked out the scientific method. Here, I have to thank all of the members of the Hong lab - Afsoon Moktar, Bathri Vajravelu, Tareq Al-Maqtari, and Pengxiao Cao, all of whom have taught me lab techniques, introduced me to new ideas, and have of course been great fun to converse with. You know you are in a great lab when, without planning it, every single person shows up at 8 PM on a Saturday and turns what would have been a long night of work into an exciting and motivating environment.

I also have to thank Dr. Hong for his help throughout my research experience. From day one, Dr. Hong was challenging me to think harder, to search deeper, and to develop my scientific skills. Throughout my investigations, he encouraged me to experiment with and explore any number of crazy ideas that one of us might have had, and always gave me solid advice when I was stuck. For this dedicating mentoring I will always be grateful.

Other thanks go to members of the University of Louisville Department of Cardiology, including Dr. McCracken, who taught me everything I know about flow cytometry, and to Dr. Jones, who provided me a number of useful microscopy tips.

Finally, I have only the biggest of hugs for my long-suffering parents, who had to oh-so-many times watch me dash off with their car at some inappropriate hour of the night to tend to my cells. They have been hugely supportive of my interests in biomedical research, and have always encouraged me to pursue my research ambi-

tions. I hope I can make them proud.

I sincerely hope that this will be the start of an exciting journey into scientific research Increasingly, I've come to appreciate that scientific feeling of not knowing what I am doing - after all, isn't scientific progress driven by our ignorance and our desperate desire to find out the truth? Now, unlike two and a half years ago, I think I am a little bit more prepared to handle those situations of cluelessness and helplessness; armed with tools of the scientific method and with Pubmed at my fingertips, I hope to be able to spring into the unknown and rummage out something. I'm not even close to being a scientist yet, but hopefully, this represents a good first step.

Contents

List of Figures

Chapter 1

Introduction

1.1 Clinical Context

Heart failure is a major public health problem, both in the United States and around the world; indeed, an estimated 5.1 million Americans have heart failure, and one in nine death certificates attribute heart failure as a cause of death [1]. Cardiomyocyte deficiency, often the result of cardiovascular disease, underlies one of the leading causes of heart failure. For example, myocardial infarction (MI) can result in loss of 25% of ventricular cardiomyocytes within several hours after onset of disease [2, 3]. Diseases of cardiac overload, such as hypertension, also activate numerous pathways for apoptosis, necrosis, and autophagy of cardiac tissue, leading to slow death of cardiomyocytes over a number of years [2, 4]. Loss of cardiomyocytes is not solely the outcome of cardiac pathologies; studies have shown that aging alone is associated with a loss of $\sim$1 g of myocardium per year [5]. In the context of an aging population, there is thus a need to investigate and assess the mechanisms underlying

cardiac damage and repair.

Loss of cardiomyocytes results in hypertrophy of existing myocytes, often accompanied by polyploidization of cells, to try to maintain force generation and contraction [2, 5]. The response to severe damage is more complex, and involves significant tissue/matrix remodeling and cytokine recruitment of inflammatory cells [6, 7]. Fibrosis and formation of scar tissue also occurs at the injury site. These mechanisms, however, have been shown to be insufficient for recovery of cardiac function [8]. The failure of the heart to adequately respond to injury has thus led to a long-standing belief that the heart is incapable of regeneration [7].

1.2 Can the Heart Regenerate?

In contrast to the traditional viewpoint of the heart as a post-mitotic or terminally differentiated organ, a great deal of recent evidence has suggested that the adult mammalian heart possesses some, albeit limited, renewal capacity [9, 10, 11, 12, 13, 14, 15, 16, 17, 18, 19, 20, 21, 22]. A highly novel study by Bergmann et al. [9] measured carbon-14 levels incorporated into genomic DNA of patient myocardial cells after aboveground nuclear bomb tests during the Cold War. Bomb tests resulted in a worldwide pulse of ^{14}C, which was incorporated into plants through photosynthesis and subsequently into humans that ate labeled plants. Following the Limited Nuclear Test Ban Treaty in 1963, ^{14}C levels dropped rapidly; this provided the researchers with pulse-chase experiment conditions in which a cardiomyocyte could be dated by determining when DNA ^{14}C levels matched atmospheric levels. The authors demonstrated that many patient cardiomyocytes were younger than the patient themselves;

various computational modeling strategies demonstrated that ∼45% of patient cardiomyocytes would be renewed over the course of a lifetime. The rate of turnover was calculated as approximately 1% per year at age 20; however, the rate drops to 0.4% at age 75.

Another study by Mollova et al. [10] presented similar results. In this study, cardiomyocytes were dissociated from hearts of patients aged 0 - 59 who had passed away of non-cardiovascular-related conditions. The samples were then analyzed by immunohistochemistry staining for phospho-histone H3 (PHH3, a mitotic marker) and mitotic kinesin-like protein (MKLP-1, a centralspindlin component required for completion of cytokinesis). The authors determined that myocyte turnover is 100% per year at age 0, but drops to 1.9% at age 20 and 0.04% for subjects older than 40. Moreover, cardiomyocyte number in the left ventricle increases 3.4 fold in the first 20 years of life. These results correspond well to calculations determined by Bergmann et al. [9]. Furthermore, the results validate that cardiomyocyte renewal occurs throughout life; however, the rate of renewal decreases with aging and may be a contributive factor in poor heart regeneration in the elderly [5].

There has, however, been controversy in terms of calculating rates of cardiomyocyte renewal in patients without cardiovascular disease. In particular, Kajstura et al. have reported significantly higher rates of cardiac renewal in healthy adult mammalian hearts [11, 12, 13]. In one study, similar to that conducted by Mollova et al., the authors analyzed immunohistochemistry for Ki67, PHH3, and aurora B kinase (three frequently used mitotic markers) in cardiomyocytes derived from hearts of patients aged 19 to 104 years. They calculated that annual rate of myocyte turnover in

females was approximately 10% at age 20 and slightly lower in men; moreover, they demonstrated turnover rates of approximately 32 - 40% for patients aged 100 [11]. According to these results, all of the myocytes of the heart are replaced between 11 and 15 times from 20 to 100 years of age. In another study, Kajstura et al. performed ^{14}C dating to calculate that the myocyte component of the heart is replaced entirely approximately 8 times over the course of an individual's life [12]. These results stand in stark contrast to the more modest rates of cardiac renewal predicted by Bergmann et al. and Mollova et al. and have invited scrutiny. Indeed, the rates calculated by Kajstura et al. are on par with proliferation rates of cell types such as cardiac fibroblasts and endothelial cells [12, 14]. Some have argued that a substantial portion of the predict myocyte turnover may be attributable to phenomena such as polyploidization (a possibility that will be considered later) or multinucleation [14]. Nevertheless, these studies taken as a whole all point to the capacity of the healthy adult heart to undergo cardiomyocyte renewal throughout life. The results of these various studies are summarized in Figure 1.1.

Cardiac renewal is not limited to the healthy heart; indeed, studies have shown some, if minimal, regenerative response in cardiomyopathy as well [12, 15, 16]. In hearts of patients who had died within 4 - 12 days of myocardial infarction, mitotic figures and newly formed cardiomyocytes were identified adjacent to the infarct, with lower rates of renewal identified at regions further from the infarct zone [15]. In particular, these cardiomyocytes identified at the peri-infarct region have been shown to be small and generally mononucleated, suggesting cardiomyogenesis [16].

Thus, there is significant evidence to suggest that the view of the heart as a static,

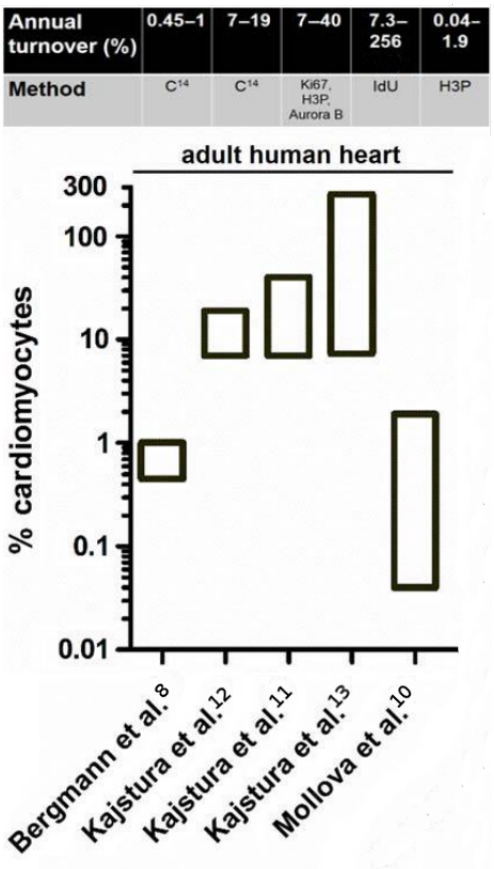

Figure 1.1: Summary of recent literature values for annual cardiomyocyte turnover. A variety of methods have been utilized in the literature, including ^{14}C labeling and immunohistochemistry analysis of tissue sections, to demonstrate cardiomyocyte renewal *in vivo*. While there are still discrepancies between various reported values of cardiomyocyte renewal, there is general acceptance that the heart possesses some, albeit limited, renewal capacity. Figure adapted from [14] under a Creative Commons 3.0 CC-BY license.

non-regenerative organ is outdated; renewal occurs both under normal physiological and disease conditions. Practical evidence from clinical experiences show that these

innate strategies of cardiac turnover are insufficient to prevent or fully ameliorate cardiomyocyte loss due to aging and cardiovascular disease. However, understanding the mechanisms underlying cardiomyocyte renewal may uncover avenues for potential future therapeutics for loss of cardiomyocytes and development of heart failure.

1.3 Do Cardiomyocytes Proliferate?

Two hypotheses have been put forward to explain how cardiomyocyte renewal occurs *in vivo*: proliferation of existing cardiomyocytes and differentiation of stem cells into cardiomyocytes [14, 17, 23]. The latter mechanism has been pursued with great enthusiasm, motivated in large part by the discovery of a variety of progenitor-like populations resident to or mobilizing to the myocardium [24, 25, 26]. Here, however, the role of cardiomyocyte proliferation is considered.

There is precedence in non-mammalian species for considering cardiomyocyte proliferation as a mechanism for cardiac renewal and repair. For example, newts and other urodele amphibians have been shown to undergo cardiac regeneration via cardiomyocyte proliferation [27, 28]. These organisms can survive and recover from excision of up to 50% of ventricle. Oberpriller et al. identified mitotic figures occurring adjacent to the damaged area, suggesting dedifferentation/proliferation of existing cardiomyocytes [27]. Another classic model of cardiomyocyte proliferation is the zebrafish [29, 30]. Zebrafish can fully recover from excision of 20% of ventricular mass within two months, replacing the wound with newly generated cardiomyocytes rather than scar tissue [29]. In an elegant fate-mapping study, Kikuchi et al. identified proliferation of existing cardiomyocytes as being responsible for cardiac recovery

[30]. In this experiment, the researchers generated a transgenic zebrafish in which a tamoxifen-inducible Cre-mediated recombination event would induce consitutive expression of green fluorescent protein (GFP) reporter in pre-existing cardiomyocytes. Thus, following excision of the ventricle, a progenitor cell-mediated recovery would result in the generation of GFP^- cardiomyocytes, while renewal from existing cardiomyocyte proliferation would produce GFP^+ cardiomyocytes. It was found that following ventricular resection, the majority of regenerated ventricular apex was GFP^+, supporting a cardiomyocyte proliferation-hypothesis for cardiac regeneration in zebrafish. Interestingly, it was found that zebrafish with mutations in proliferation pathways underwent fibrosis and scar formation similar to that found in adult mammals following cardiac injury [29]. These results suggest that fibrosis of cardiac tissue is a response to inhibition of or lack of vigor in cardiomyocyte proliferation.

Zebrafish heart structure differs somewhat from mammalian heart. For example, mammalian hearts are four-chambered with double-circulation, while fish hearts are two-chambered with single circulation. Fish hearts also generally pump blood with lower force, which may affect cardiomyocyte physiology. Moreover, the majority of zebrafish cardiomyocytes remain mononucleated throughout life, while mammalian cardiomyocytes become binucleate (and often multinucleate) shortly after birth [31]. However, a number of studies have shown that neonatal mammal hearts retain proliferative capacity throughout development and shortly after birth [22, 31, 32]. Cardiomyocyte proliferation plays a key role in heart development during embryogenesis [31]. Moreover, in mice younger than 7 days of age, excision of up to 15% of ventricular myocardium is met with full recovery within two months and minimal scarring [22].

Fate mapping studies similar to those conducted in zebrafish identify proliferation of existing cardiomyocytes as being responsible for cardiac regeneration. Investigators identified cardiomyocytes near the injured area with myofibrillar breakdown characteristic of cardiomyocyte dedifferentiation and proliferation [22, 32]. After 7 days of age in mice, however, cardiac injury does not result in cardiomyocyte regeneration; instead, fibrosis and scar formation occurred [22]. This loss of regenerative potential coincides with the binucleation of mammalian cardiomyocytes in early development. Thus, mammalian cardiomyocytes have proliferative capacity throughout embryogenesis and until shortly after birth, but this capacity may be inhibited or downregulated in a large portion of myocytes in the first week after birth.

The extent to which adult mammalian cardiomyocytes retain proliferation capacity has been highly controversial. A number of studies have documented the presence of mitotic figures (via immunhistochemistry analysis of mitotic markers such as phospho-histone H3, Ki67, and others) in both normal and diseased cardiac tissue [12, 13, 15, 16, 19, 20]. In particular, Beltrami et al. have shown that the number of myocytes positive for Ki67 increase significantly in hearts isolated from patients who died shortly after myocardial infarction; these mitotic figures were largely clustered around the infarct area [15]. Contrastingly, Hesse et al. reported that following infarction, cardiomyocytes bordering the infarct region do not undergo mitosis [33]. Here, the authors utilized annilin, a component of the contractile ring with characteristic subcellular localization during mitosis, as a marker of cell division. The researchers analyzed cardiomyocytes in eGFP-annilin transgenic mice and found no evidence of proliferation following injury. Several groups have sought to address the discrepancies

between these findings [14, 17, 32]. Indeed, analysis of cardiomyocyte proliferation is complicated by a number of experimental challenges, including unambiguously identifying cardiomyocytes from other cell types, differentiating between mitosis and other phenomena (such as polyploidization/endoreduplication), and identifying what may be rare mitotic events. These issues are considered in more detail later. The potential role that stem and progenitor cells may play in adult mammalian cardiac renewal and regeneration must also be considered. Hsieh et al. performed an elaborate fate-mapping analysis to demonstrate the role of stem cells in replenishing cardiomyocytes following infarction. In this study, the researchers used doubly-transgenic mice to generate tamoxifen-inducible expression of GFP reporter protein in 82.7% of pre-existing cardiomyocytes [21]. During normal aging of up to one year, the proportion of GFP^+ cardiomyocytes did not change, suggesting that any renewal under healthy conditions occurred without input from non-cardiomyocyte cell types. However, following injury, the percentage of GFP^+ cardiomyocytes dropped to 67.5% near the infarct zone, suggesting replacement of cardiomyocytes from some progenitor source. In a similar fate-mapping study, Malliaras et al. identify cardiomyocyte proliferation as being the primary mechanism of cardiac renewal under healthy conditions in adult mammalian heart, but show that progenitor cell recruitment is the predominant mechanism of recovery following injury [16]. In this model, normal renewal is mediated by a small, constantly cycling population of uninucleate cardiomyocytes. These cells, however, are insufficient to regenerate the heart during conditions of injury, resulting in recruitment of progenitors to the infarct area. Though these results suggest a key role of stem cell recruitment in ameliorating cardiac injury, they do not conclusively rule

out the possibility of cardiomyocyte proliferation during injury response. Taken as a whole, these results support the possibility that cardiomyocyte proliferation occurs in the adult mammalian heart, albeit at rates too small to sufficiently regenerate the heart following age- or disease-mediated cardiomyocyte loss.

1.4 Factors Regulating Cardiomyocyte Proliferation

The fact that adult mammalian cardiomyocytes may maintain proliferative capacity has led to an interest in investigating mechanisms regulating proliferation. Thus far, a number of genes, miRNAs, proteins, and transcription factors have been shown to be involved in controlling and/or inducing cardiomyocyte proliferation, including SV40 large T antigen [18, 31, 34]; c-myc [18]; homeobox gene *MeisI* [35]; miR-195, miR-590-3p, miR-199a-3p, and miR-133a [31, 36]; Hippo signalling pathway [31]; cyclins and cyclin-dependant kinases [18, 31]; FOXO1 and FOXO3 transcription factors [37]; and others. Moreover, the modes of regulation have shown to be both negative and positive [31]. The tremendous variety of pathways and machinery involved in the regulation of cardiomyocyte proliferation suggest that it is a highly controlled phenomenon that is activated and inhibited by a number of temporal cues throughout development and maturation.

The possibility that cardiomyocytes may proliferate has generated investigation into induction of proliferation as a therapeutic approach. To this end, a number of cocktails of growth factors have been developed to promote cardiomyocyte prolifer-

ation [17, 18, 31, 38, 39, 40, 41, 42]. Engel et al. proposed the inhibition of p38 mitogen-activated protein kinase (p38 MAPK) as an avenue for inducing cardiomyocyte proliferation [17, 40, 41]. Through a combination of p38 MAPK inhibitor (p38 MAPKi) and fibroblast growth factor 1 (FGF1) treatment, the researchers were able to induce gene expression corresponding to dedifferentiation and cell-cycle re-entry in cardiomyocytes in culture [40]. Moreover, FGF1/p38 MAPKi therapy resulted in increase in phosphorylated histone-3 staining and cell number in culture, with cardiomyocytes demonstrating sarcomeric dedifferentiation characteristic of proliferative cardiomyocytes. In another study, Bersell et al. identified the tyrosine kinase receptor ErbB4 as playing a role in myocardial regeneration *in vivo*; in particular, inactivation of ErbB4 results in reduced cardiomyocyte regeneration following infarct, while high ErbB4 expression corresponds to improved cardiac regeneration [38, 39]. The authors utilized the growth factor neuregulin1 (NRG1), an agonist of the ErbB4 receptor, to promote cardiomyocyte cell division *in vitro* [39]. Interestingly, the authors found that NRG1 induced proliferation in mononucleate myocytes, but not in binucleate or multinucleate myocytes. This may suggest that, developmentally, multinucleation acts an inhibitor of cardiomyocyte proliferation [31]. In a third study, Kühn et al. utilized periostin, an activator of cardiomyocyte membrane integrins, to induce proliferation [42]. All three therapies, when utilized *in vivo* following myocardial infarction, improved cardiac function and regeneration and reduced fibrosis [39, 41, 42]. However, it is not fully clear whether cardiomyocyte proliferation is the main source of improved cardiac function. While all three approaches show convincing induction of cell-cycle gene expression and increase in staining for various mitotic markers in

culture, each therapy also promotes angiogenesis *in vivo*, which may suggest reasons for cardiac improvement following infarction other than just proliferation of existing cardiomyocytes. These therapeutics provide hope that targeting pathways involved in regulation of cardiomyocyte proliferation may serve as alternative therapeutic avenues to cell therapy [17]. However, the *in vivo* results demonstrate the need for an assay to unambiguously demonstrate myocyte proliferation in animal models.

1.5 Challenges in Assessing Cardiomyocyte Proliferation

Identifying cardiomyocyte mitosis *in vivo* is an endeavour filled with a number of major experimental challenges [14, 17, 32]. First and foremost, the architecture of cardiac tissue makes it challenging to correctly identify cardiomyocytes in tissue sections, even when stained with cardiomyocyte-specific cytoplasmic markers. Several authors have shown that cardiomyocytes display irregular shape *in vivo*, with a number of fibroblasts and inflammatory cells found in spaces between cardiomyocytes [32, 43]. In a particularly critical study, Ang et al. compared conventional confocal microscopic analysis of cardiomyocyte tissue sections (with and without a membrane marker) to a gold standard of a transgenic mouse in which nuclear-localized -galactosidase report was expressed only in cardiomyocytes, with >99% of cardiomyocytes labeled thus [43]. The authors found that conventional methods could misidentify cardiomyocytes up to 10% of the time. A number of techniques have been utilized to try and improve fidelity of cardiomyocyte identification, including labeling cardiomyocyte nuclei with

markers such as Nkx2.5 or various transgenic mice models [21, 32, 44]. Others have aimed to use labour-intensive dispersion techniques to specifically isolate cardiomyocytes from tissue samples prior to analysis [9, 19]. These methods have improved accuracy of identification of cardiomyocytes; however, considerations of tissue architecture and the presence of proliferative non-myocyte cells must be taken into account when determining proliferation of cardiomyocytes.

Two particularly popular tools for assessing proliferation are bromodeoxyuridine (BrdU) and Ki67, shown in Figure 1.2. BrdU is synthetic analogue of thymidine in which a methyl group of thymidine is replaced by a bromine group. During S phase of the cell cycle, cells replicate DNA. When pulsed with BrdU during this period, cells may incorporate BrdU into DNA instead of thymidine; subsequently, immunohistochemistry can be utilized to identify cells that have undergone DNA synthesis (see Figure 1.2a). Ki67 is nuclear protein thought to be associated with cell proliferation and ribosomal RNA transcription. Ki67 is known to be expressed through all active stages of cell cycle (though not during quiescent states such as G_0); however, while during interphase expression is within the cell nucleus, Ki67 expression relocates to the chromosomal surface upon initiation of M-phase (see Figure 1.2b). The predictability and general ease of use associated with BrdU and Ki67 have made them popular markers for proliferation in various cancers [45]. Likewise, both have been used in a number of studies to assess cardiomyocyte proliferation. However, unlike most cancers, cardiomyocytes are known to undergo abortive variants of cell-cycle such as endocycle (in which DNA synthesis occurs without subsequent mitosis) and endoreduplication (in which mitosis is initiated but cytokinesis does not occur)

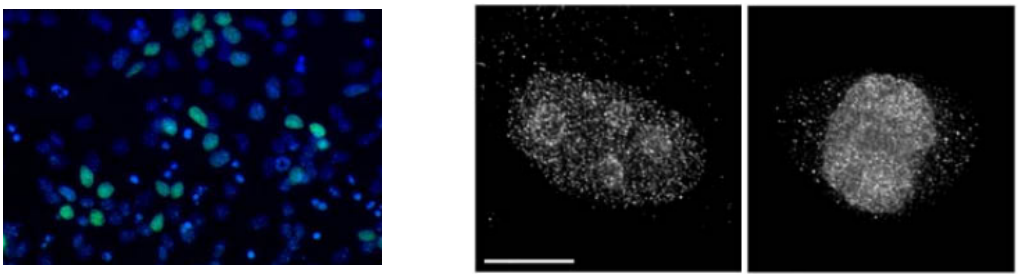

(a) BrdU (b) Ki67

Figure 1.2: (a) BrdU labeling (green) of primary E12 mouse cortex cells. BrdU is a thymidine analogue, and is thus incorporated into the DNA of cells undergoing DNA synthesis when provided in the culture media. Taken from [46]. (b) Ki67 labeling of HeLa cells. In interphase cells *(left)*, Ki67 shows a diffuse nuclear localization; however, upon onset of mitosis *(right)*, Ki67 localization changes to the surface of chromosomes. Taken from [47] under license from Springer Science. While both BrdU and Ki67 have been popular proliferation markers, they fail to unambiguously distinguish between mitosis and abortive cell cycle.

[18, 32]. The net result of these phenomena may be increased DNA content and ploidy in the cell or increased numbers of nuclei per cell without actual cell division. Neither BrdU nor Ki67 distinguish between these various cell cycle variants and actual completion of mitosis, making them poor markers to assess cardiomyocyte proliferation.

Some researchers have aimed to compensate for the issue of ambiguity by utilizing markers that closely correspond to progress through and termination of mitosis. For example, phospho-histone H3 (PHH3) has been frequently used as a marker of mitosis *in vitro*[48]. Phosphorylation of histone H3 (which occurs site-specifically at serine

10 on the histone protein) occurs almost exclusively during mitosis. Moreover, the intensity and localization of phosphorylation can often be used to track progression of the cell throughout each phase of mitosis (see Figure 1.3a). Thus, antibody staining of cells allows for an accurate assessment of proliferation [48]. Mitotic kinesin-like protein (MKLP-1) has also been used as a marker for mitosis. MKLP-1 is a component of the centralspindlin complex, a key part of the contractile ring of cytokinesis [49]. Thus, immunostaining for MKLP-1 allows identification of cells about to undergo cytokinesis and complete mitosis (see Figure 1.3b). A third approach utilizes anillin to track progression through mitosis. Anillin is a scaffolding protein that, like MKLP-1, plays a role in mediating cytokinesis [33]. The localization of anillin within the cell can be used to track cell cycle; in particular, anillin localizes to the contractile ring in early cytokinesis and to the midbody in late cytokinesis (see Figure 1.3c). In this sense, anillin can also unambiguously mark cells undergoing mitosis. These three markers are shown in Figure 1.3. However, cardiomyocytes *in vivo* undergo mitosis very rarely [14, 32]. For example, using MKLP-1, Mollova et al. report that in cardiomyocyte samples derived from patients aged 0 - 1, $0.016 \pm 0.003\%$ of cardiomyocytes were found to be in cytokinesis; this number drops to $0.005 \pm 0.005\%$ for subjects in the second decade of life [10]. The authors identified no myocytes in cytokinesis past age 20. These extremely small numbers, coupled with relatively high standard deviations, indicate the extreme rarity of mitotic cardiomyocytes found *in vivo*. Markers such as as PHH3, MKLP-1, and anillin, while allowing for unambiguous identification of mitosis, provide only snapshots in time. Given that mitosis itself comprises only a relatively small portion of cell cycle, markers must be devised to al-

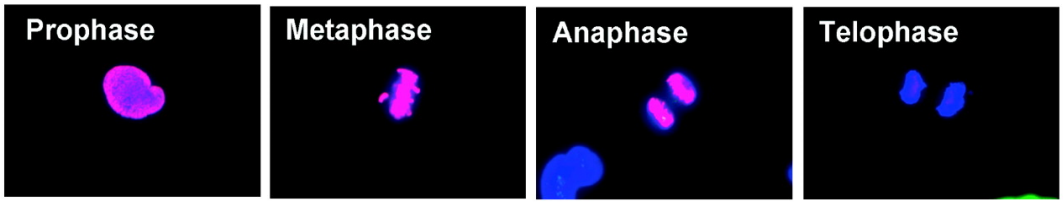

(a) PHH3

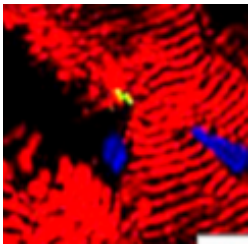

(b) MKLP-1

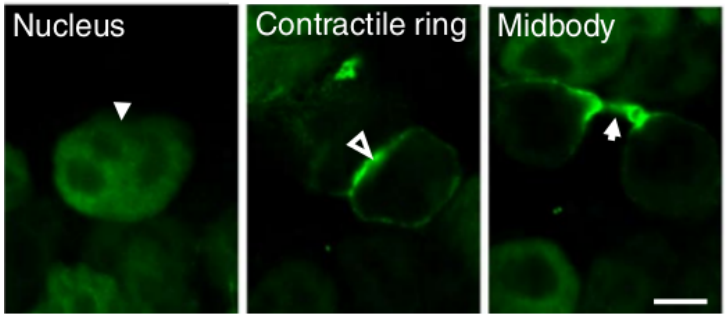

(c) Anillin

Figure 1.3: Examples of PHH3, MKLP-1, and anillin labeling. (a) PHH3 labeling (red) of HeLa cells in various stages of mitosis. Taken from [50] under license from the American Association of Cancer Research. (b) MKLP-1 labeling (green). MKLP-1 forms a key part of the contractile ring during cytokinesis. Taken from [10].(c) Anillin labeling (green). In interphase, anillin localizes to the nucleus; however, as mitosis occurs, it localizes first to the contractile ring and then to the midbody. Taken from [33] under a Creative Commons 2.5 BY-NC license. While these three markers unambiguously mark mitotic events, their short half-life following mitosis makes them inefficient for tracking what may be extremely rare mitotic events in cardiomyocytes.

low for sensitive analysis of cardiomyocyte proliferation *in vivo*.

These challenges highlight the need for a new method of detecting cardiomyocyte proliferation. In particular, such a tool must be easily visualized and/or quantified,

unambiguous, and integrative in nature. Here, a potential molecular probe that satisfies these criteria is described.

1.6 ndCKAP2 as a Probe for Proliferation

Cytoskeleton-associated protein 2 (CKAP2) may serve as a potential probe for assessing cardiomyocyte proliferation *in vivo*. CKAP2 has been shown to play a number of key roles in regulating mitosis [51, 52, 53, 54]. In particular, CKAP2 has been shown to have microtubule-stabilizing properties and is responsible for maintenance of mitotic spindle bipolarity [51]. Moreover, CKAP2 is a known substrate for the anaphase-promoting complex/Cdh1, suggesting a key role for the protein in mitotic spindle dynamics [52]. Overexpression and/or mutation of CKAP2 can result in a number of microtubule abnormalities and spindle defects in mitosis [52]. CKAP2 has been shown to be upregulated in a number of malignant cancers, while knockdown *in vitro* has resulted in reduction of rate of cell growth [53].

Similar to mitotic markers such as PHH3, MKLP-1, and anillin, the localization of CKAP2 corresponds well to progression through cell cycle (Figure 1.4). During interphase, CKAP2 is primarily associated with microtubules. In the early stages of mitosis, CKAP2 is similarly associated with spindle microtubules. However, at cytokinesis, CKAP2 translocates to the midbody microtubules and the nuclei of the newly forming daughter cells [51, 52]. Shortly after mitosis, this translocated CKAP2 is broken down by the anaphase-promoting complex in a ubiquitin ligase-mediated proteolysis pathway [52]. The unambiguous change in localization of CKAP2 throughout mitosis, and particularly during cytokinesis, has led to some investigators utilized

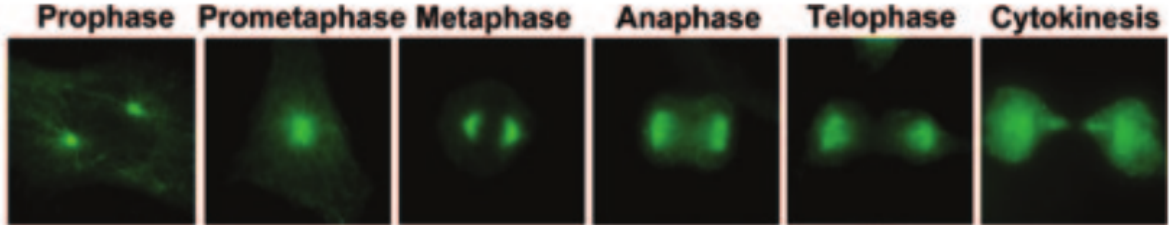

Figure 1.4: Localization of CKAP2 throughout cell cycle. In prophase, CKAP2 is found with a cytoplasmic localization, and is strongly associated with microtubules. After completion of mitosis, however, CKAP2 becomes nuclear in localization. Taken from [52].

CKAP2 as a mitotic probe for studying proliferation in samples from breast cancer patients [54]. However, like some of the above markers, CKAP2 only identifies cells *as they are undergoing mitosis* rather than cells that have *already undergone mitosis*; it is not integrative in nature.

In studying the interaction between CKAP2 and the anaphase-promoting complex, Hong et al. identified a destruction motif in CKAP2 that is recognized by Cdh1 for CKAP2 breakdown following completion of mitosis [52]. This motif, named the KEN box after the three residues comprising the structure, is conserved across higher eukaryotes and involved in the ubiquitin ligase-mediated degradation of CKAP2. By mutation of the three residues to alanine, Hong et al. generated a mutant which resisted breakdown following mitosis (Figure 1.5). This mutant, named non-degradable CKAP2 (ndCKAP2), presents a cytoplasmic localization during interphase. Upon completion of mitosis, however, the protein translocates to nucleus in an easily visualized and unambiguous manner. Moreover, because the nuclear ndCKAP2 is not

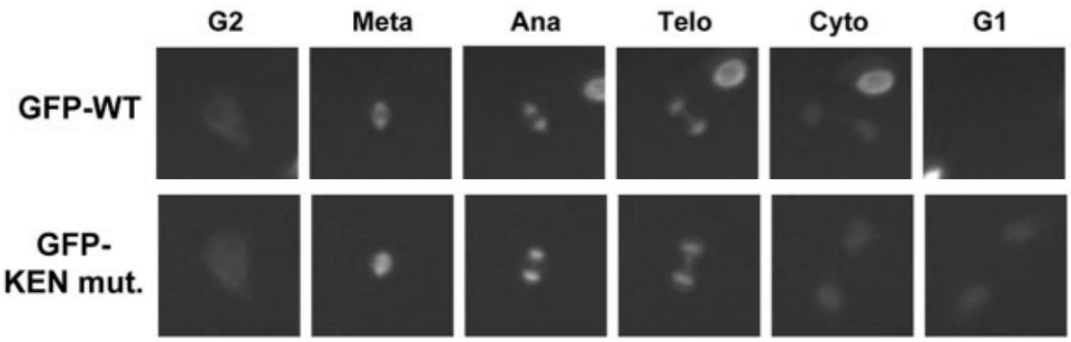

Figure 1.5: Comparison of CKAP2 (WT) and ndCKAP2 (KEN mutant). While CKAP2 is degraded within thirty minutes after completion of mitosis via ubiquitin-mediated pathways, nuclear ndCKAP2 is not broken down. Taken from [52].

broken down after completion of mitosis, it makes it possible to identify not just cells that are undergoing mitosis at the time of analysis, but cells that have undergone mitosis. In this sense, ndCKAP2 serves as an integrator for mitotic events occuring in tissue. Given these characteristics, ndCKAP2 may be an appropriate tool for mitotic experiments, including the investigation of cardiomyocyte proliferation *in vivo*. The present study aims to establish ndCKAP2 as a valid and useful molecular probe for assessing proliferation in a visualizable, unambiguous, and integrative manner.

1.7 Hypothesis and Aims

It is hypothesized that ndCKAP2 can serve as an easily visualized, unambiguous, and integrative molecular probe for assessing proliferation. This hypothesis will be tested in three aims:

- **Generation of a fluorescent cell division probe.** A genetic construct for an eGFP-ndCKAP2 fusion protein will be engineered, and a lentiviral-based expression system carrying this construct will be generated. These constructs will be tested by either transfection or viral transduction of both HeLa and HEK293 (two common transformed cell lines) cells and neonatal rat ventricular cardiomyocytes (NRCMs, a primary cell line).

- **Validation of ndCKAP2 as an unambiguous marker of proliferation.** Cell-cycle studies in proliferative cells will be used to quantifiably assess whether ndCKAP2 remains cytoplasmic in quiescent cells and translocates to the nucleus solely following completion of mitosis.

- **Determination of the half-life of nuclear ndCKAP2.** It is presumed that at some point nuclear ndCKAP2 is broken down or exported from the nucleus, if very slowly. Given that a novel aspect of the ndCKAP2 probe is its ability to persist in the nucleus following completion of mitosis, it is necessary to know how long this persistence will last. Calculation of the half-life of ndCKAP2 once translocated into the nucleus (and comparison with other commonly used probes) will be used as a metric to assess the integrative nature of ndCKAP2.

The goal of the current study is to demonstrate the use of ndCKAP2 as a powerful tool for measuring proliferation. It is believed that the characteristics of ndCKAP2 will make it an ideal probe for addressing the controversy of cardiomyocyte proliferation under physiological and post-injury conditions, and will be the focus of future investigations.

Chapter 2

Materials and Methods

2.1 Genetic Constructs and Lentiviral Production

Generation of an enhanced green fluorescent protein (eGFP) fusion ndCKAP2 construct (pEGFP-C2 ndCKAP2) has been previously described [52]. The eGFP-ndCKAP2 coding sequence was PCR amplified with Pfu DNA polymerase (Agilent) using the following primers: Forward - 5' CACCATGGTGAGCAAGGGCGAG 3'; Reverse - 5' TTATGTTGTATCAGCCTCATAGTACACCCG 3'. The amplification cycle was: 95°C (30 sec) → 60°C (15 sec) → 72°C (3 min), repeated for 25 cycles. This produced DNA with a CACC sequence at the 5' end. The purified PCR-amplified product was then subcloned into pLenti6/V5 vector harboring human cytomegalovirus (CMV) promoter and rous sarcoma virus (RSV) enhancer using the Directional TOPO® cloning kit (Invitrogen) as per the manufacturer instructions. In this system, an overhang in the cloning vector (GTGG) charged with topoisomerase recognizes and invades the 5' end of the PCR product; thus, subcloning can

be performed with high efficiency without addition of a ligase. Identity of construct was assessed by investigating products of BamHI/XhoI and SmaI restriction enzyme digests on an agarose gel. Sequencing was also performed at DNA Core (University of Louisville School of Medicine) to verify fidelity of construct. To generate additional construct for introduction into cells, pLenti6-eGFP-ndCKAP2 was used to transform competent Stbl3 E. coli. DNA was subsequently harvested via Miniprep or Midiprep kits (Qiagen). All other constructs used in experimentation, such as GFP-C2 control, were obtained from Dr. Kyung Hong at the UofL Department of Molecular Cardiology.

To generate lentivirus for expression of eGFP-ndCKAP2 in primary mammalian cell lines, the ViraPower^{TM} Lentiviral Expression System was used according to manufacturers instructions. 293FT cells were transfected using Lipofectamine 2000 (Invitrogen) with pLenti6-eGFP-ndCKAP2 along with an optimal viral packaging mix containing pLP1, pLP2, and pLP/VSVG plasmids (provided by manufacturer). Virus-containing supernatant was harvested 72 hours later and titered prior to use.

2.2 Cell Culture, Transfection, and Transduction

HeLa, HEK293, and NIH3T3 cells were cultured in Dulbecco's modified Eagle's medium (DMEM) containing 10% fetal bovine serum (FBS) and penicillin/streptomycin. Neonatal rat ventricular cardiomyocytes (NRCMs), isolated from 1 - 2 day old Sprague-Dawley rats, were graciously provided by Dr. Steven Jones at the UofL Department of Molecular Cardiology. NRCMs were cultured in DMEM containing 5% FBS, penicillin/streptomycin, and Vitamin B12. In addition, during the first 2 - 3 days of

culture, NRCMs were incubated with 0.1 mmol/L BrdU to prevent outgrowth of any contaminating fibroblasts. Human cardiac stem cells (CSCs) were graciously provided by Matthew Keith at the University of Louisville Department of Molecular Cardiology, and were isolated based on c-Kit expression from endocardial biopsies from consenting patients with ischemic cardiomyopathy. CSCs were cultured in F12 media containing 10% FBS, 2.5 units erythropoietin, 10 ng/mL basic fibroblast growth factor (bFGF), and 0.2 mM glutathione. Cells were maintained in a humidified culture incubator at 37°C with 5.0% CO2. Proliferative cells (HeLa, HEK293, NIH3T3, and CSCs) were subcultured every 2 - 3 days.

Transfection of cells was performed using Lipofectamine 2000 following the manufacurer's instructions. Liposome-DNA complexes were removed five hours after transfection. Lentiviral transduction was performed by mixing virus (titered in DMEM) with polybrene (Sigma) and adding to cells. During viral transduction, cells were cultured in DMEM containing 10% FBS without antibiotics. 24 hours after transduction, cells were washed and media was changed to DMEM containing 10% FBS and penicillin/streptomycin.

2.3 Cell Cycle Synchrony

To synchronize cells in S-phase, a single thymidine block was performed. Cells were transfected five hours prior to initiation of the block. Cells were then incubated with 2 mM thymidine (Sigma, dissolved in PBS) for 20 hours. Subsequently, the cells were washed thrice with warmed PBS and released into fresh media to be assayed. In some experiments, a tighter synchrony was desired, and thus a double thymidine

block was performed instead. To perform double thymidine block, cells were incubated with 2 mM thymidine for 19 hours. Subsequently, the cells were washed thrice with warmed PBS and released into fresh media for 9 hours. During the last five hours of this release, cells were transfected. The cells were then blocked a second time with 2 mM thymidine. Cells were then washed thrice with warmed PBS and released into fresh media to be assayed.

To synchronize cells in G_2/M boundary, a thymidine-nocodazole block was performed. Cells were transfected five hours prior to initiation of the thymidine block. Cells were then incubated with 2 mM thymidine for 20 hours. Subsequently, the cells were washed thrice with warmed PBS and released into media containing 1 μM nocodazole (Sigma, dissolved in DMSO). After 12 hours, warmed media was used to detach rounded mitotic cells from the culture plate by gentle pipetting. Cells were then re-plated in fresh media to be assayed.

2.4 Immunofluorescence Staining and Imaging

Cells grown on glass cover-slips were fixed in 3.7% formaldehyde solution in PBS for 10 minutes at room temperature, and subsequently permeabilized in 0.5% Triton-X-100 in PBS for 10 minutes. Following incubation in a blocking solution of 5% bovine serum albumin in PBS for 30 minutes, cells were incubated with primary antibody (diluted in blocking solution) for 1 hour at room temperature. Cells were then washed thrice with PBS and incubated with the secondary antibody (diluted in blocking solution) for 1 hour at room temperature. Cells were then washed thrice with PBS and counterstained with DAPI. Coverslips were mounted on glass slides with Fluo-

romount (TM) aqeuous mounting medium (Sigma). Primary antibodies were diluted as follows: GFP (Abm), 1:300; PHH3 (Millipore), 1:2000; and α-tubulin, 1:1000. All Alexa-fluor conjugated secondary antibodies were acquired from Invitrogen and used at a dilution of 1:1000.

Images were collected using either an EVOS fluorescent cell imaging system (Life Technologies) or an Axiovision fluorescent microscope (Carl Zeiss). Images were analyzed using ImageJ software and manipulated and overlaid using the open-source Gnu Image Manipulation Program (GIMP). For calculations based on fluorescence, the following formula was used to correct signal for background and determine a value of fluorescence per unit area (FPUA) in a given region:

$$\text{FPUA} = \frac{\text{Integrated Density} - \text{Cell Area} \times \text{Mean Fluorescence of Background}}{\text{Cell Area}}$$

2.5 Flow Cytometry and FACS Analysis

Cells were fixed in cold 70% ethanol overnight or longer. Prior to analysis, cells were washed with PBS containing 1% bovine serum albumin and subsequently stained in a propidium iodide (PI) solution containing 50 g/mL PI, 0.1% sodium citrate, 0.3% NP-40, 100 μg/mL RNase A, 1% bovine serum albumin, and PBS for 20 minutes at room temperature. PI is a DNA dye, and thus serves visualize progression through cell cycle. Profiles of PI-stained cells were obtained using a FASCalibur system (Becton Dickinson) and analyzed using FlowJo software (Tree Star). Cells were sequentially gated based on SSC-A vs FSC-A, FSC-W vs FSC-H, and SSC-W vs SSC-H to discriminate against doublets or debris, as well as on GFP expression.

Chapter 3

Results

3.1 Generation of pLenti6-eGFP-ndCKAP2

eGFP-ndCKAP2 was PCR amplified from a previously generated construct [52] and subcloned into pLenti6/V5 vector using the Directional TOPO® cloning kit (Invitrogen). This strategy obviated the need for a ligase to mediate the subcloning process. The vector map of pLenti6-eGFP-ndCKAP2 (referred to from here as GFP-ndCKAP2) is shown in Figure 3.1.

To validate the identity of the construct, GFP-ndCKAP2 was subject to restriction enzyme digest; the products of the digest were subsequently analyzed through agarose gel electrophoresis. In the first reaction (outlined in Figure 3.2a), GFP-ndCKAP2 was subject to digest from the restriction enzymes BamHI and XhoI. The sites of cleavage for BamHI and XhoI are found on the pLenti6 vector flanking the insert; an additional XhoI cut site is found between the GFP and ndCKAP2 open reading frames. Thus, when run on a gel, this reaction should produce three fragments - a

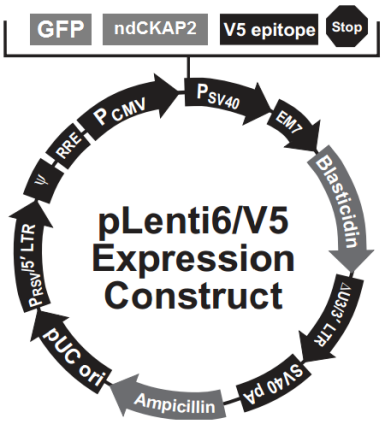

Figure 3.1: Vector map of pLenti6-GFP-ndCKAP2. The plasmid was engineered by subcloning the GFP-ndCKAP2 open-reading frame into the lentiviral vector through the use of the TOPO®cloning kit (Invitrogen).

7.0 kilobase (kb) fragment corresponding to the pLenti6 vector, a 2.0 kb fragment corresponding to the ndCKAP2 sequence, and a 0.7 kb fragment corresponding to the eGFP sequence. Thus, the BamHI/XhoI digest served to validate the insertion of both the fluorescent protein GFP and the proliferation marker ndCKAP2 into the pLenti6 vector.

The purpose of the second digest (outlined in Figure 3.2b), performed utilizing the restriction enzyme SmaI, was to validate the orientation of the GFP-ndCKAP2 insert into pLenti6 vector. The target cleavage sequence for SmaI is found within the ndCKAP2 open reading frame as well as within the vector. In the case that the insert was in the correct orientation, restriction enzyme digest would produce an 8.1 kb fragment and a 1.6 kb fragment. However, if the insert orientation were reversed, the digest would produce a 7.8 kb fragment and a 1.9 kb fragment.

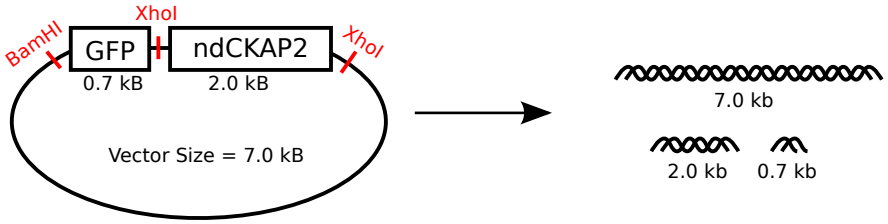

(a) BamHI/XhoI restriction enzyme digest

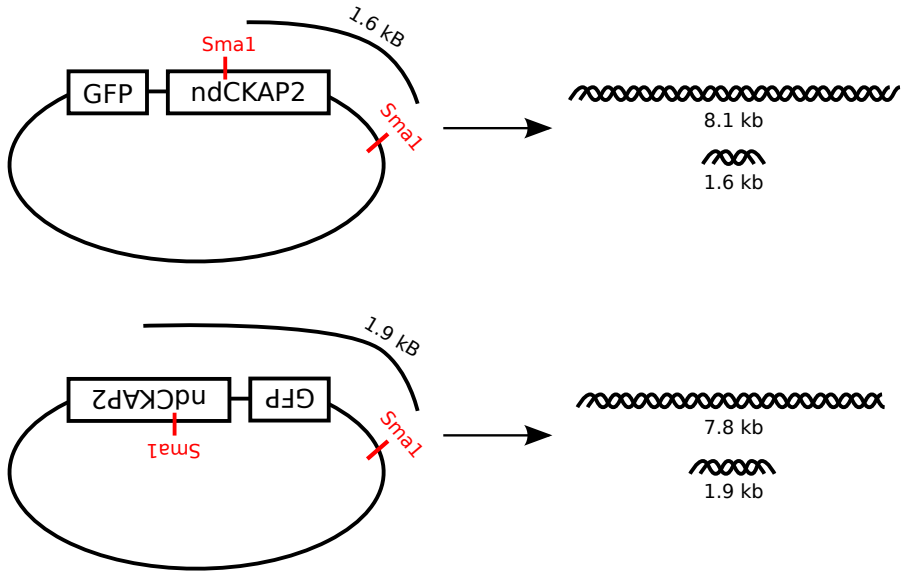

(b) Sma1 restriction enzyme digest

Figure 3.2: Schematics of Restriction Enzyme Experiments. In (a), the construct is subject to BamHI/XhoI digest; this allows for verification that the GFP and ndCKAP2 open reading frames were inserted into the vector. In (b), the construct is subject to SmaI digest to verify if the insert is in the correct orientation *(top)* or reversed *(bottom)*.

Figure 3.3 shows the results of the restriction enzyme digests. The column labeled **1** and **2** served as control cases, and represent digest with BamHI and XhoI alone, respectively. Column **3** shows the results of BamHI/XhoI digest; as can be seen, the expected fragment sizes are observed, validating the inclusion of both GFP and ndCKAP2 into the pLenti6 vector. Column **4** shows the results of SmaI digest. As can be seen, the resultant fragment sizes match the predicted values shown in Figure 3.2b, verifying that the GFP-ndCKAP2 fusion protein was inserted into the pLenti6 vector in the correct orientation.

While restriction enzyme digests allow for general validation of subcloning, several other aspects of the GFP-ndCKAP2 fusion protein had to be assessed prior to ap-

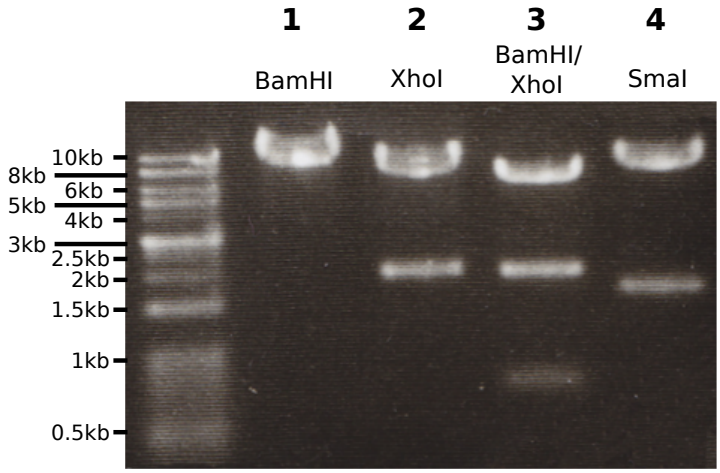

Figure 3.3: Analysis by restriction enzyme digest of pLenti6-GFP-ndCKAP2. Columns **1 - 4** represent digest with BamHI alone, XhoI alone, BamHI/XhoI, and SmaI respectively. Comparison with Figure 3.2 validates the successful generation of the lentiviral vector.

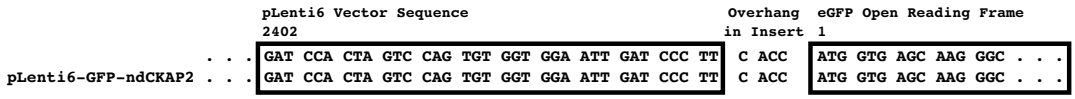

Figure 3.4: Sequencing of pLenti6-GFP-ndCKAP2 at the 5' end of the GFP-ndCKAP2 insert. The top row represents expected sequences of the pLenti6 vector and wild-type eGFP open reading frame. The numbers represent the base pair position along the sequence. In the engineering pLenti6-GFP-ndCKAP2, a CACC overhang generated in the insert is invaded by a corresponding sequence in the pLenti6 vector. As can be seen, the sequences of the engineered vector match with the expected sequences; moreover, the eGFP protein remains in frame. Further sequencing demonstrated the absence of point mutations in the engineered construct (not shown here).

plication. First, it was necessary to ensure that the GFP-ndCKAP2 coding sequence had been inserted in the correct reading frame (or whether a frameshift mutation had occurred during the subcloning process). Secondly, the construct needed to be evaluated to ensure that no point mutations had occurred. To validate these two aspects, GFP-ndCKAP2 was sequenced. Figure 3.4 shows a comparison of the pLenti6 vector as well as the eGFP open reading frame to the GFP-ndCKAP2 insert at the site of insertion into the vector. As can be seen, the GFP-ndCKAP2 insert is maintained in frame. Sequencing also demonstrated the absence of point mutations from the final GFP-ndCKAP2 vector (results not shown here).

These results validate the subcloning of the GFP-ndCKAP2 fusion protein con-

struct into the lentiviral vector. This vector was subsequently transfected into 293FT cells, along with a mix of genes for viral packaging proteins, to generate lentivirus carrying the GFP-ndCKAP2 expression construct.

3.2 GFP-ndCKAP2 can be expressed in tranformed and primary cell lines

To determine whether the engineered GFP-ndCKAP2 successfully produced expression of the fusion protein in cells, HeLa cells were transfected with the GFP-ndCKAP2 construct and subsequently analyzed via immunohistochemistry. CKAP2 is known to have microtubule-stabilizing properties during mitosis, and remains closely associated with the microtubules and cytoskeletal structure of the cell through interphase and the early stages of mitosis [51, 52]. To verify this association, HeLa cells transfected were stained with α-tubulin, a structural subunit of microtubules, after transfection. As can be seen in Figure 3.5, cytoplasmic GFP-ndCKAP2 localization corresponds well to α-tubulin expression in the cell. Subsequently, the protein translocates to the nucleus, as is verified by staining for DAPI, a DNA dye. Representative examples of both nuclear and cytoplasmic ndCKAP2 are seen in Figure 3.5.

To test expression of the GFP-ndCKAP2 fusion protein, three commonly used immortalized cell lines (HeLa, HEK293, and NIH3T3) were transfected with the GFP-ndCKAP2 construct (Figure 3.6). Similarly, HEK293 cells as well as two primary cell lines (CSCs and NRCMs) were transduced with the lentivirus carrying the GFP-ndCKAP2 expression construct (Figure 3.7). All cell types tested readily express the

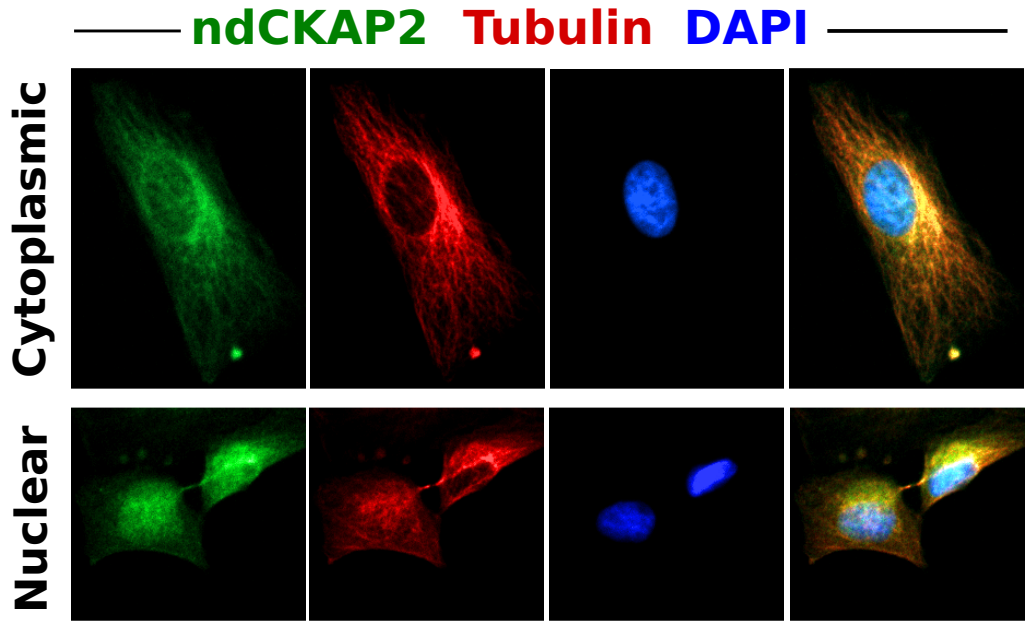

Figure 3.5: Subcellular localization of GFP-ndCKAP2. In the cytoplasmic localization *(top)*, ndCKAP2 shows strong association with microtubules, as visualized by α-tubulin staining. The nuclear localization *(bottom)* is verified by co-staining with DAPI (a nuclear dye).

fusion protein GFP-ndCKAP2; moreover, this expression can be readily visualized under fluorescent microscopy. Initially, all cells express GFP-ndCKAP2 with a cytoplasmic localization. However, within one day of expression, all proliferative cell types (HeLa, HEK293, NIH3T3, and CSCs) demonstrated cells with nuclear localization of GFP-ndCKAP2. Examples of cytoplasmic and nuclear localization of the fusion protein are shown in higher magnification the insets of Figures 3.6 and 3.7. In contrast, cells with nuclear GFP-ndCKAP2 were not seen in NRCMs, as would be expected of a cell type that does not proliferate *in vitro*.

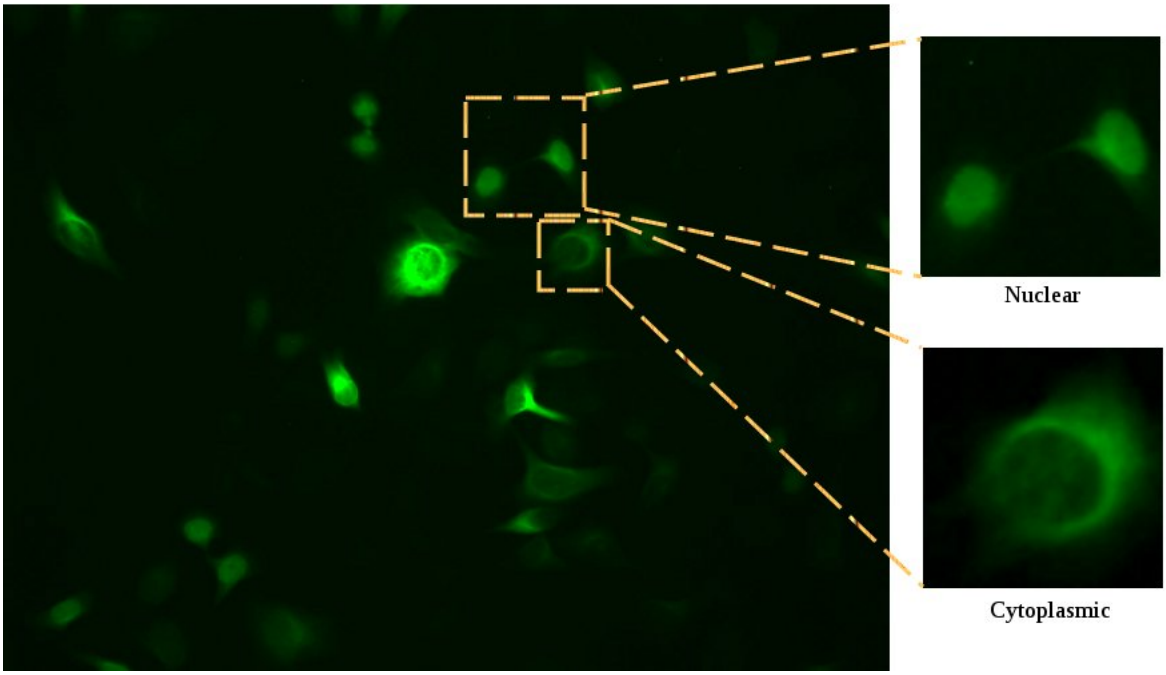

(a) HeLa cells tranfected with GFP-ndCKAP2.

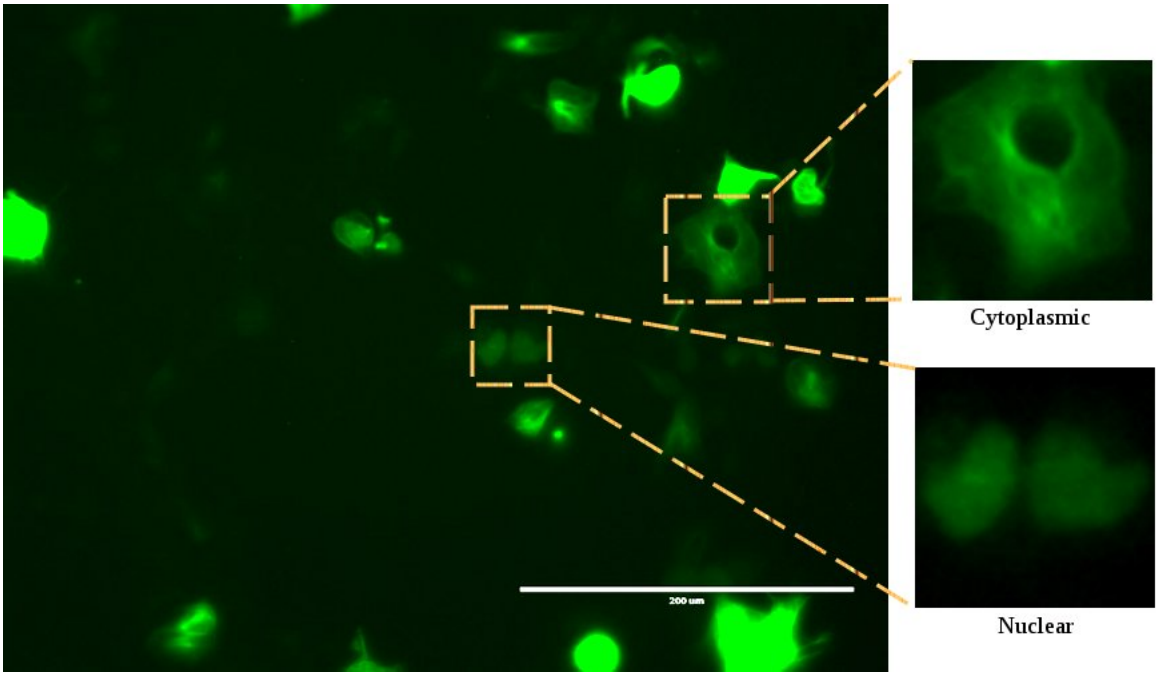

(b) HEK293 cells transfected with GFP-ndCKAP2.

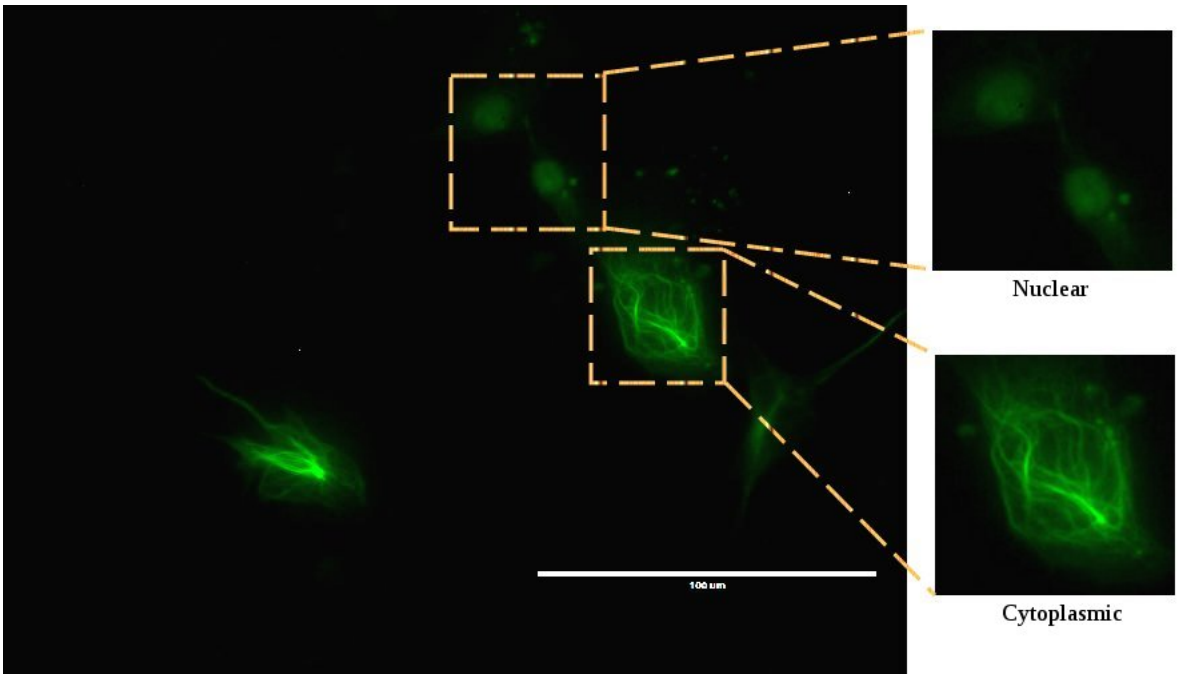

(c) NIH3T3 cells transfected with GFP-ndCKAP2

Figure 3.6: HeLa, HEK293, and NIH3T3 cells transfected with GFP-ndCKAP2. In all cells, expression is clear and readily visible within 24 hours of transfection. All cell types demonstrated cells with nuclear localization of ndCKAP2 within one day of onset of expression. Insets show examples of cells with both cytoplasmic and nuclear localization of GFP-ndCKAP2.

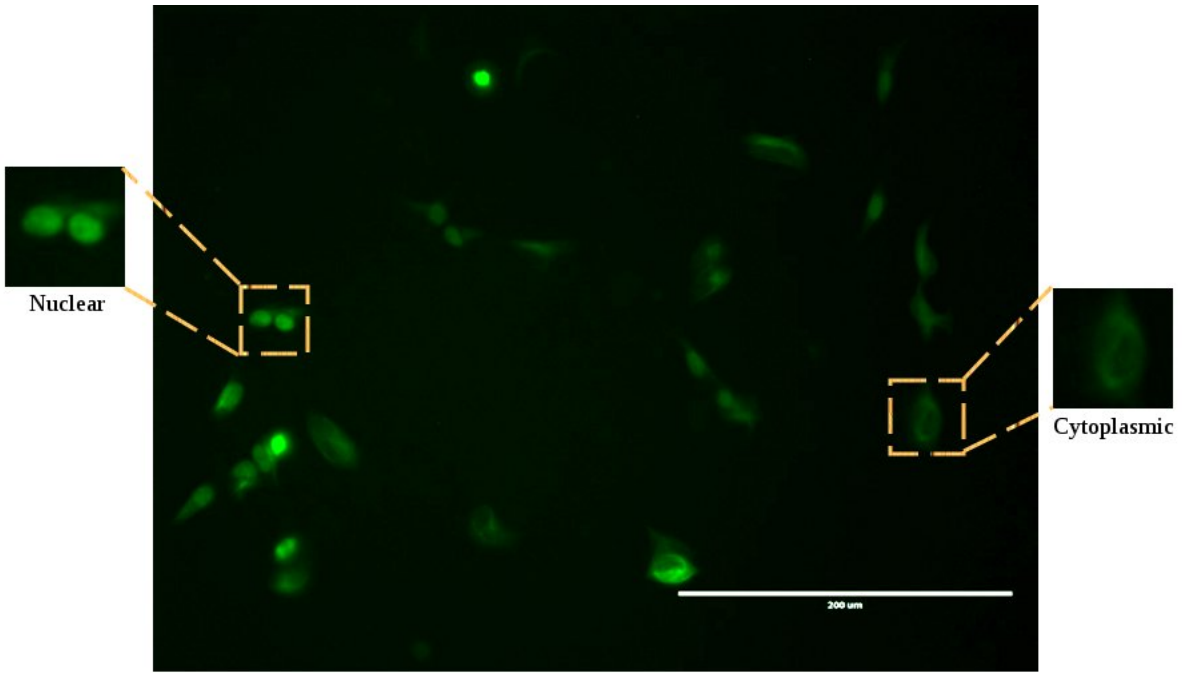

(a) HEK293 cells transduced with GFP-ndCKAP2-carrying lentivirus.

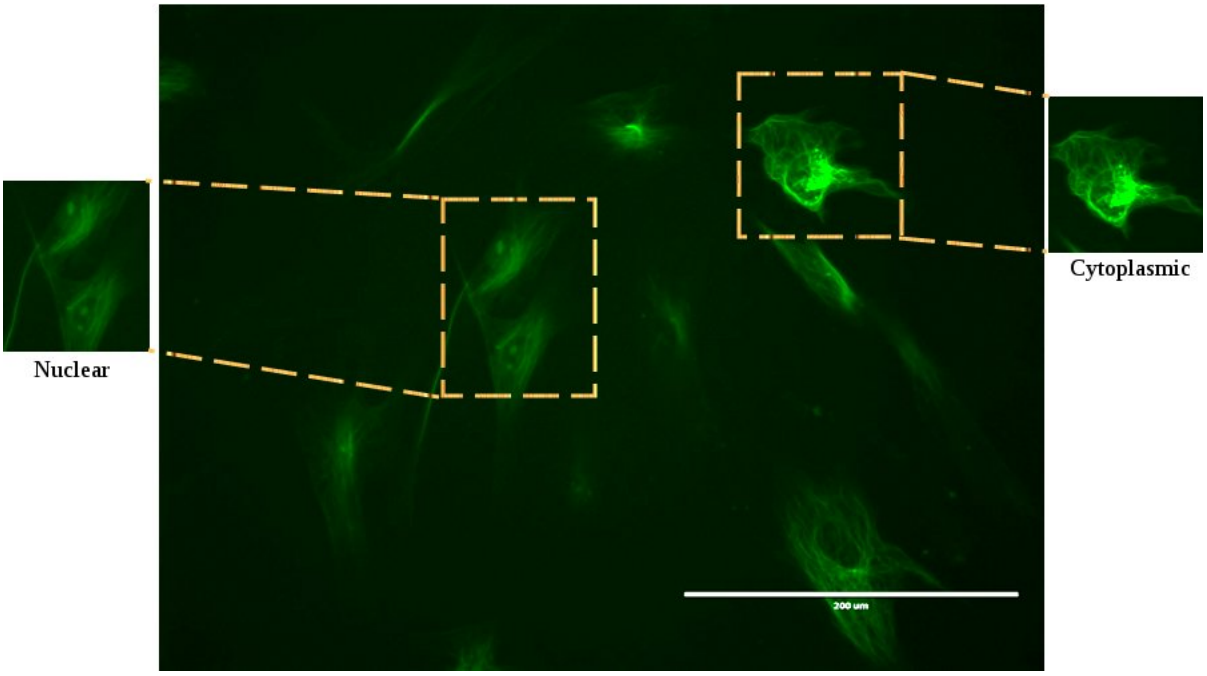

(b) CSCs transduced with GFP-ndCKAP2-carrying lentivirus.

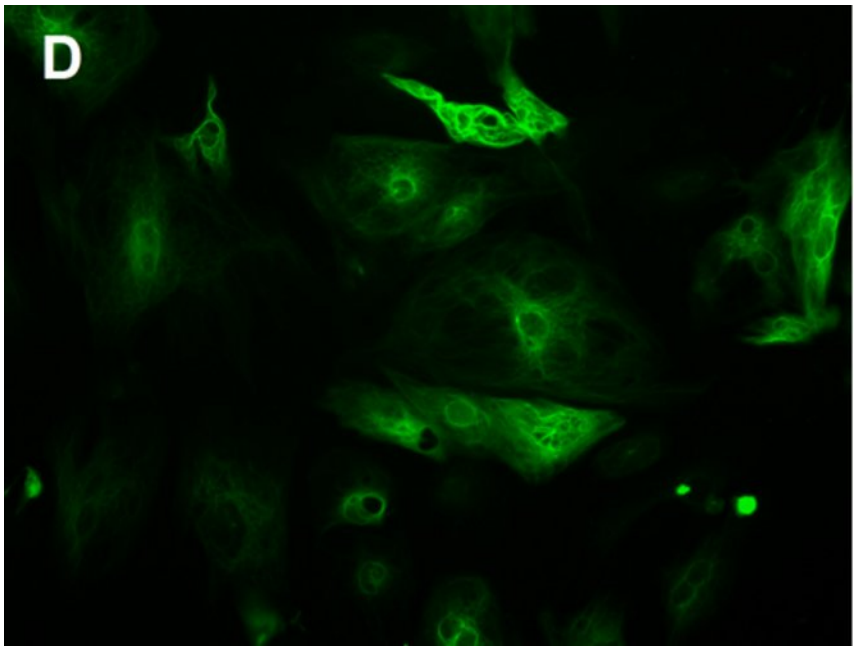

(c) NRCMs transduced with GFP-ndCKAP2-carrying lentivirus.

Figure 3.7: HEK293 cells, CSCs, and NRCMs transduced with GFP-ndCKAP2-carrying lentivirus. Expression is clear and readily visible within 48 - 72 hours post-transduction. Nuclear localization of ndCKAP2 was seen in HEK293 cells and CSCs after expression of GFP-ndCKAP2, as seen in the insets. However, quiescent NRCMs do not demonstrate nuclear ndCKAP2 even after a week in culture, supporting the claim that ndCKAP2 only translocates to the nucleus following completion of mitosis.

These experiments validate the expression of GFP-ndCKAP2 in both immortalized and primary cell lines (by both liposome-mediated transfection and lentiviral transduction). Moreover, the cytoplasmic localization was verified in all cell types and shown to be microtubule-associated, and the presence of nuclear-localized GFP-ndCKAP2 was noted in all proliferative cell types.

3.3 Appearance of nuclear ndCKAP2 corresponds with completion of mitosis in synchronized cells

To quantitatively validate that nuclear GFP-ndCKAP2 serves as an unambiguous marker of proliferation, the appearance of nuclear ndCKAP2 was tracked in HeLa cells synchronized by double thymidine block. Figure 3.8a shows a schematic of the double thymidine experiment. After double thymidine block, cells were synchronized at the G_1/S border (Figure 3.8b). After release, the cells synchronously proceeded through cell cycle, entering into G_2 phase at approximately 6 hours, and completing mitosis between 8 - 12 hours. Progression of HeLa cells transfected with GFP-ndCKAP2 through cell cycle after double thymidine block is visualized by flow cytometry analysis of PI staining, shown in Figure 3.8c. The percentage of cells in G_1, S, and G_2/M phases respectively was quantified using computational analysis based on built-in cell cycle progression models in FlowJo, and plotted in Figure 3.8d. As can be seen by the increase in percentage of the number of cells in G_1 phase at 14 hours, approximately 31.3% of cells re-entered and progressed through cell cycle following release from double thymidine block. To further demonstrate progression through cell cycle, cells were harvested at 4, 6, 8, 10, and 12 hours post-release and stained with PHH3; representative images are shown in Figure 3.8e.

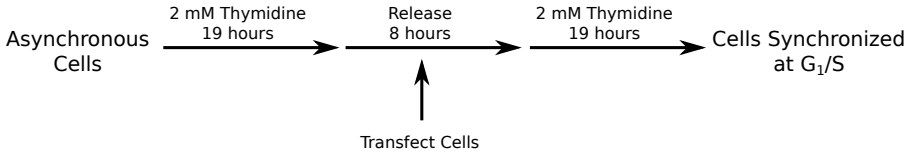

(a) Schematic of double thymidine experiment.

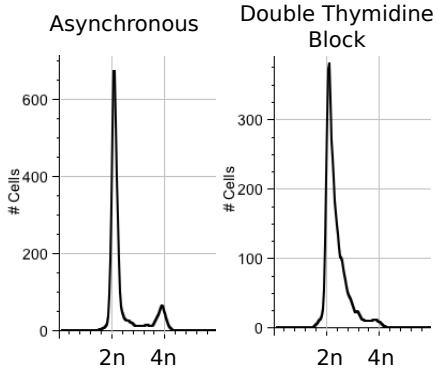

(b) PI staining profile for asynchronous cell population *(left)* and population synchronized at G_1/S by double thymidine block *(right)*.

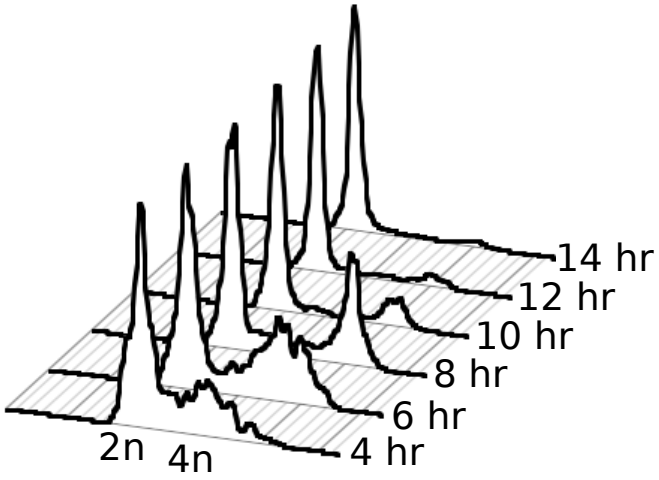

(c) PI staining profile for synchronous cell populations released from double thymidine block.

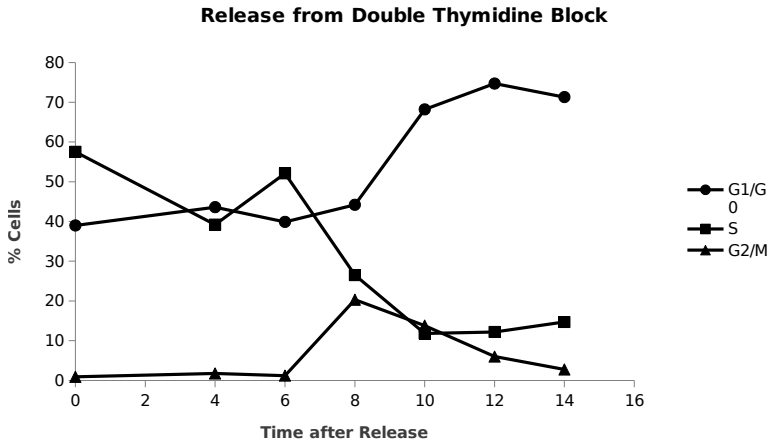

(d) Cell cycle analysis for synchronous cell populations released from double thymidine block. Time in hours.

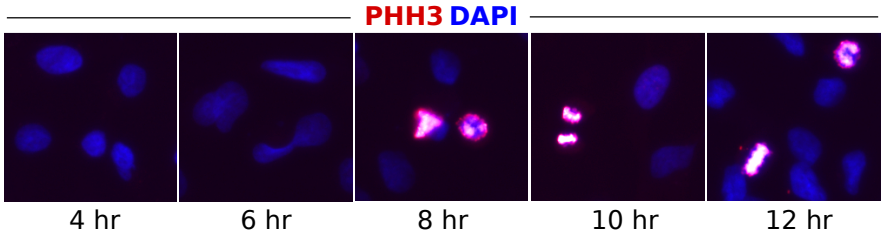

(e) PHH3 (red) staining at serial-time points following release from double thymidine block. Overlaid on DAPI (blue)

Figure 3.8: Progression of HeLa cells through cell cycle following synchronization through double thymidine block. (a) Schematic of the double thymidine block experiment. After completion of both sequential blocks, >99% of cells are arrested in G_1/S; release from the block causes cells to progress synchronously through cell cycle. (b - d) Validating progression through cell cycle via PI analysis. About 30% of cells proceed synchronously through cell cycle. (e) PHH3 staining at serial time-points following release from double thymidine block. Mitotic figures begin to appear 8 hours post-release, as supported by the PI data.

Figure 3.9 shows the analysis of localization of GFP-ndCKAP2 in HeLa cells released from double thymidine block. Cells were assayed at 4, 6, 8, 10, 12, and 14 hours post-release, stained for GFP and DAPI, and visualized under fluorescent microscope. Quantification was done by assessing the number of cells expressing cytoplasmic and nuclear localization of GFP-ndCKAP2 in several random fields of view on the slide. >150 cells were counted per slide, and four slides were assayed per time point. As

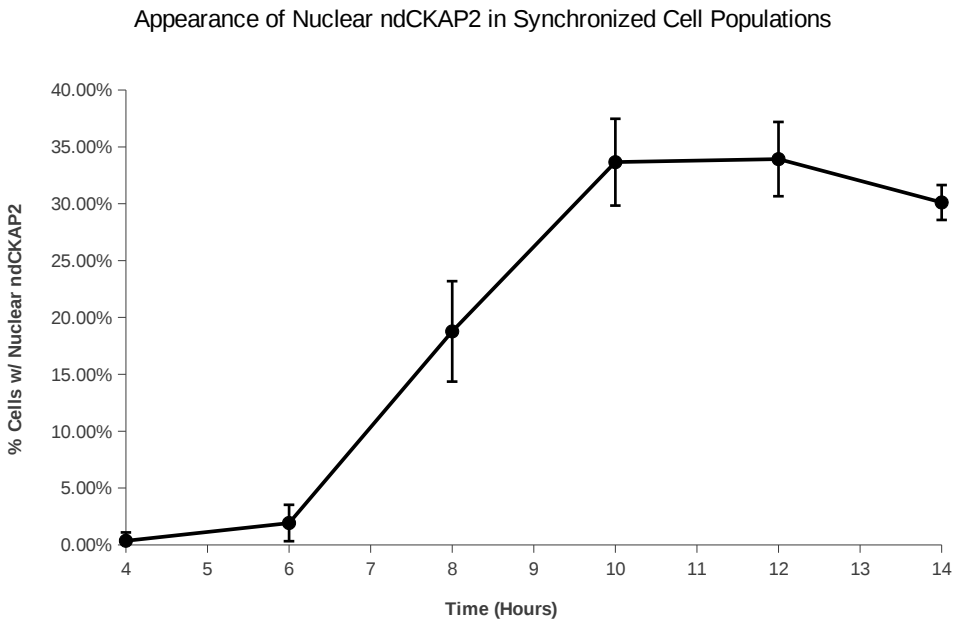

Figure 3.9: Appearance of Nuclear ndCKAP2 in HeLa cells synchronized by double thymidine block. As can be seen, very few nuclear ndCKAP2 figures appear prior to 8 hours post-release from double thymidine block. This corresponds well to the cell cycle release profiles shown in Figure 3.8. Data shown is mean ± SD, with $N = 4$ and > 150 cells counted per sample.

can be seen, increase in the proportion of cells showing nuclear localization of GFP-ndCKAP2 correlates strongly with progression through cell cycle. Very few ($\sim$ 0% of observed cells at 4 hours and <2% at 6 hours) show nuclear localization of GFP-ndCKAP2 up until 6 hours; however, a marked increase occurs between 6 and 10 hours post-release from double thymidine block. This increase also corresponds with the increase in cells staining positive for PHH3, as shown in Figure 3.8e, suggesting a connection between change in localization and completion of mitosis. At 14 hours, the percentage of cells showing nuclear localization of GFP-ndCKAP2 is 30.11% $\pm$ 1.53%, which matches the percentage of cells that progressed synchronously through cell cycle as determined by computational modeling. Figure 3.10 shows representative images of cells at various assayed time points. Visual inspection verifies the increase in cells showing nuclear GFP-ndCKAP2 starting at 8 hours post release.

To further validate that nuclear localization of ndCKAP2 occurs only after completion of mitosis, HeLa cells were synchronized at the G_2/M border by a thymidine-nocodazole block. Nocodazole interferes with polymerization of microtubules; thus, cells enter mitosis but are arrested in prometaphase. Figure 3.10a demonstrates arrest by and release from thymidine-nocodazole block, as analyzed by flow cytometry of PI-stained cells. As can be seen, cells synchronously proceed through mitosis and enter G_1 within 4 - 6 hours after release. The percentage of cells in G_1, S, and G_2/M phases respectively was quantified using computational modeling and plotted in Figure 3.10b. Figure 3.12 shows representative images of cells arrested by thymidine-nocodazole block and cells 6 hours after release. As can be seen, prior to release, most cells are rounded up and show diffuse expression of GFP-ndCKAP2

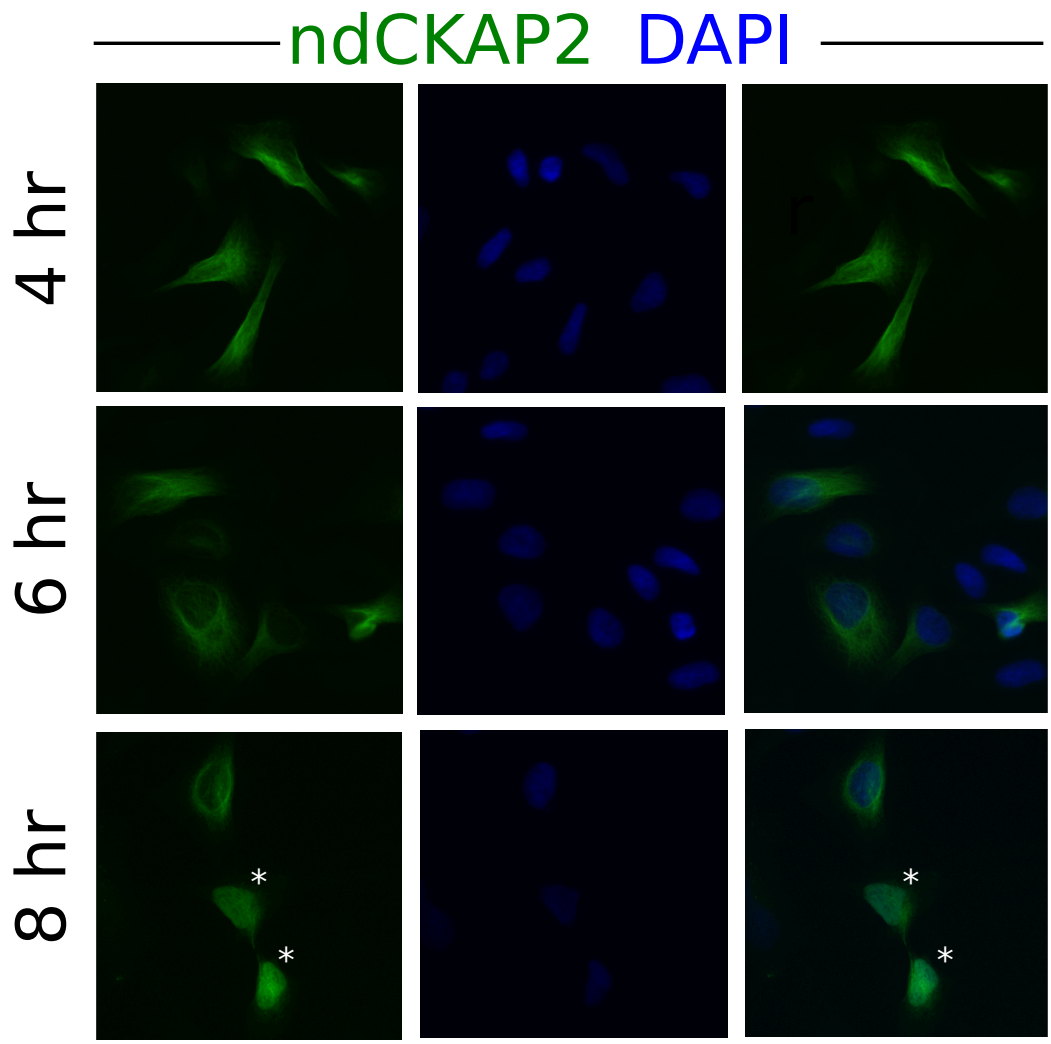

(a) 4 - 8 hours after release from double thymidine block.

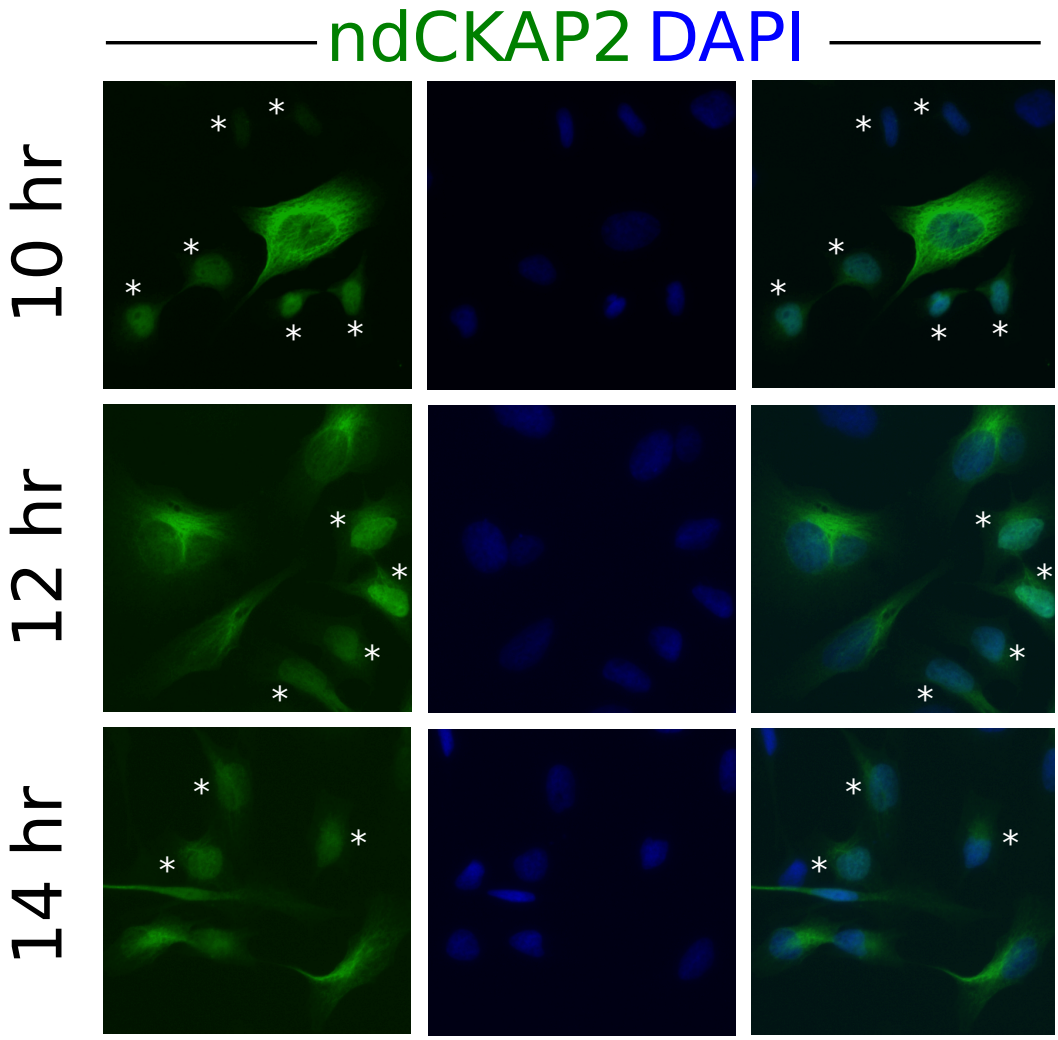

(b) 10 - 14 hours after release from double thymidine block.

Figure 3.10: Synchronized HeLa cells transfected with GFP-ndCKAP2 released from double thymidine block. As can be seen, appearance of nuclear ndCKAP2 (marked by white stars) first occurs at 8 hours post-release from double thymidine block, and is easily visualized.

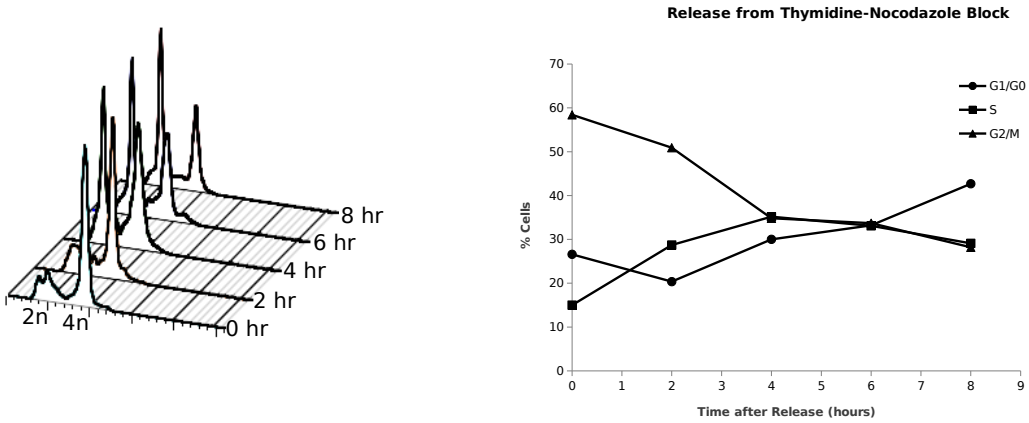

(a) PI staining profile for synchronous cell populations released from thymidine-nocodazole block.

(b) Cell cycle analysis for synchronous cell populations released from thymidine-nocodazole block.

Figure 3.11: Progression of HeLa cells through cell cycle following synchronization through thymidine-nocodazole block. As can be seen, cells arrested at G_2/M synchronously proceed through mitosis and enter G_1 within 4 - 6 hours.

throughout the cell; this expression does not correspond to DAPI staining of the nucleus. After release, however, cells demonstrating nuclear GFP-ndCKAP2 are observed. These results support the hypothesis that nuclear localization of GFP-ndCKAP2 is not a product of *onset* of mitosis, but rather of completion of mitosis.

Taken as a whole, these cell cycle experiments in synchronized HeLa cell populations demonstrate that cytoplasmic ndCKAP2 translocates to the nucleus following completion of mitosis; this translocation is unambiguous and can be used to track mitotic cells.

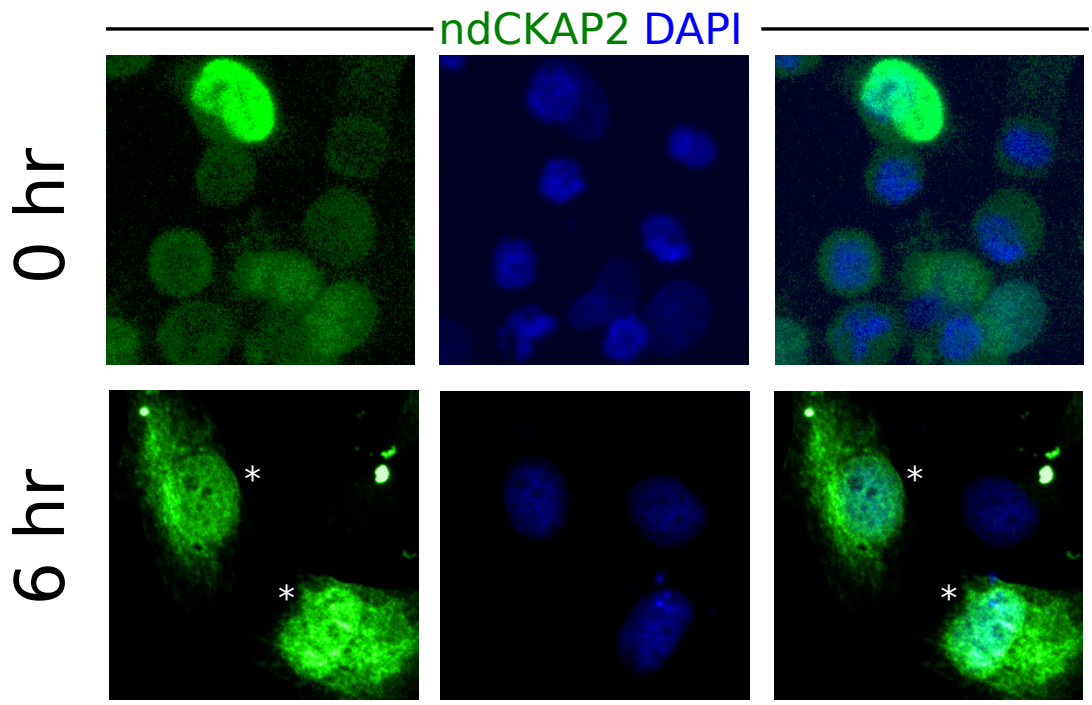

Figure 3.12: Synchronized HeLa cells transfected with GFP-ndCKAP2 before and after release from thymidine-nocodazole block. Prior to release, most cells are arrested at prometaphase due to the microtubule-inhibitory effects of nocodazole. At this point (0 hr), GFP-ndCKAP2 expression is diffuse throughout the rounded cell. After completion of mitosis, cells display nuclear GFP-ndCKAP2 (as seen at 6 hrs post-release, marked by white stars).

3.4 ndCKAP2 demonstrates a long half-life upon translocation to the nucleus

To demonstrate the integrative nature of GFP-ndCKAP2, the half-life of the nuclear-localized ndCKAP2 was calculated. A schematic demonstrating the method-

(a) Schematic of half-life experiment.

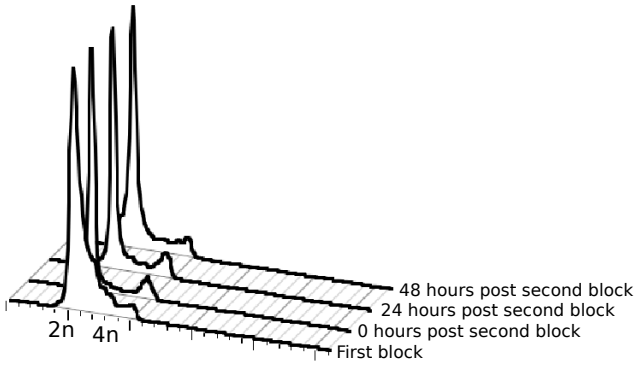

(b) PI staining profile for various intervals of the half-life experiment.

Figure 3.13: Half-life experiment cell cycle analysis. In this experiment, transfected HeLa cells were synchronized in G_1/S phase by incubation with thymidine, and then released to proceed synchronously through exactly one cell cycle. Cells were then incubated again with thymidine to prevent re-entry into cell cycle, allowing analysis of cells that had proceeded through one round of mitotic division.

ology is shown in Figure 3.13a. GFP-ndCKAP2-transfected HeLa cells were synchronized in G_1/S by a thymidine block and released until exactly one cell cycle had been completed. Subsequently, the cells were blocked from re-entering cell cycle by incubating again with thymidine. Cells were subsequently harvested and analyzed via immunofluorescence analysis. To verify the various cell cycle arrests, flow cytometry was performed on PI stained cells (Figure 3.13b). These results were validated visu-

ally as well. No nuclear-localized ndCKAP2 was seen in cells synchronized in G_1/S by the first thymidine block; however, nuclear GFP-ndCKAP2 appeared in samples harvested 12 hours after release from thymidine block. Cells subsequently blocked by the second incubation of thymidine demonstrated no new mitotic figures.

In the first method of determining half-life of the nuclear-localized ndCKAP2, the fluorescence per unit area (FPUA) of nuclei of cells demonstrating nuclear-localized ndCKAP2 was measured in cells 0 and 24 hours after initiation of the second thymidine block (i.e. after completion of one synchronous round of cell cycle). >30 nuclei were analyzed per slide, and four slides were assayed per time point. This experiment thus allowed for a comparison of protein content (assessed by fluorescence) in the cells. As can be seen in Figure 3.14, FPUA decreases 24 hours after completion of synchronous cell cycle; this decrease was found to be statistically significant ($p < 0.05$). To calculate half-life, the following equation based on a standard model of exponential decay was used:

$$FPUA(24 \text{ hrs}) = FPUA(0 \text{ hrs})\left(\frac{1}{2}\right)^{24 \text{ hrs}/t_{\frac{1}{2}}}$$

where $FPUA(N)$ represents FPUA at time N. Based on this formula and the experimentally determined values, a half-life of ~75.8 hours was determined. Representative images are seen in Figure 3.15.

One weakness of the FPUA method is that it may skew half-life in favour of high GFP-ndCKAP2 expressors. Thus, a cell population half-life was calculated to determine the time required for 50% of cells expressing nuclear ndCKAP2 after completion of one round of cell cycle to cease expression. The fraction of cells expressing nuclear-localized ndCKAP2 was determined by visualizing and counting cells harvested 0

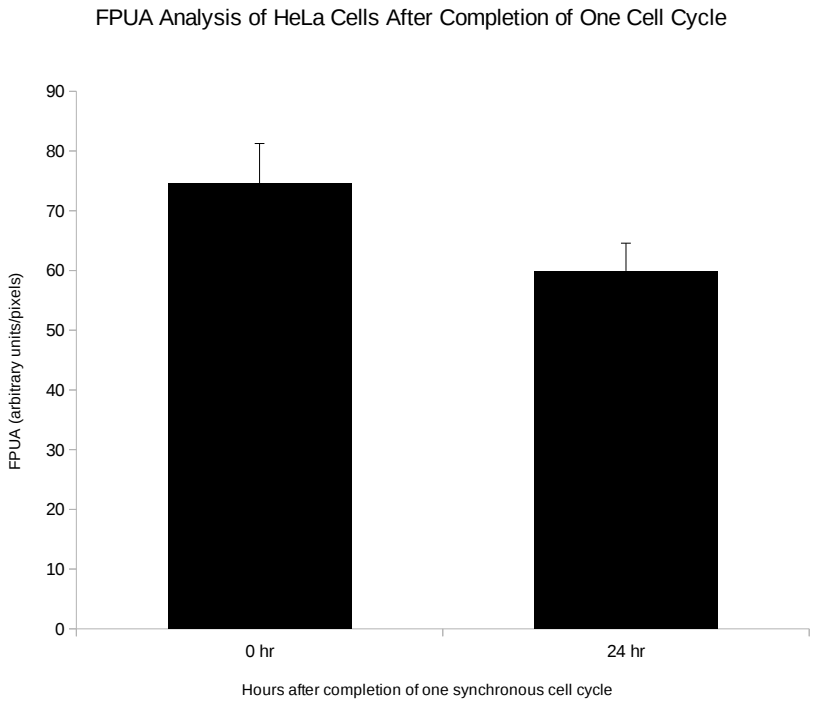

Figure 3.14: Determination of half-life of nuclear-localized GFP-ndCKAP2 in HeLa cells by FPUA analysis. Cells that had completed one synchronous cell cycle were blocked from re-entering cell cycle and analyzed. Data shown is mean ± SD, with $N = 4$ and > 30 nuclei counted per sample. The difference in FPUA between the 0hr and 24 hr groups was statistically significant ($p < 0.05$), as determined by a one-tailed Student's t-test.

and 24 hours after completion of one round of cell cycle under fluorescent microscope. >150 cells were counted per slide, and four slides were assayed per time point. As can be seen in Figure 3.16, the proportion of cells displaying nuclear ndCKAP2 decreases 24 hours after completion of synchronous cell cycle (determined to be statistically

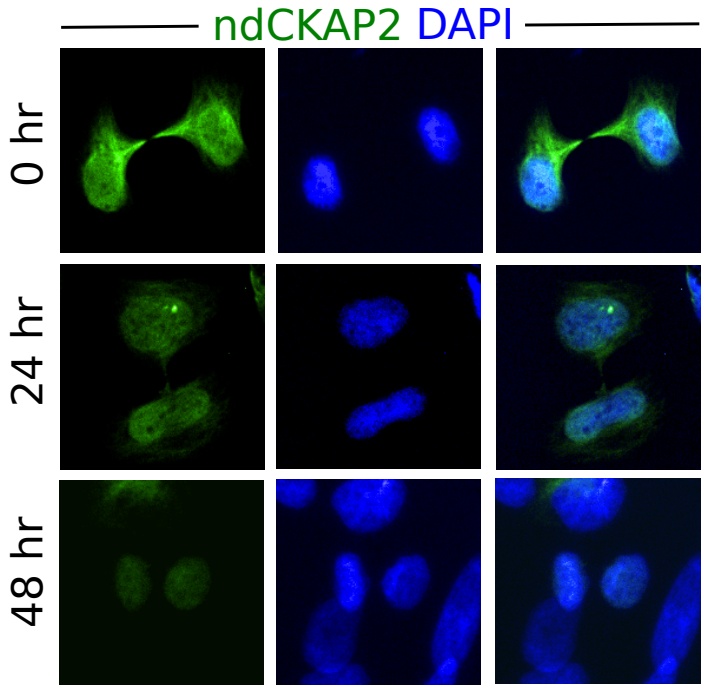

Figure 3.15: Representative images of half-life analysis of nuclear ndCKAP2 in transfected HeLa cells. As can be seen, FPUA decreases from 0 to 24 hours after completion of one synchronous round of cell cycle. Nuclear ndCKAP2 is also observed 48 hours after synchronous cell cycle, supporting the integrative nature of nuclear ndCKAP2.

significant, $p < 0.05$); however, this decrease is more pronounced than determined by the FPUA method. Based on these results and using an analogous exponential decay model similar to that used with the PFUA method, the cell population half-life of nuclear ndCKAP2 was determined to be ∼15.84 hours. These findings suggest that while nuclear ndCKAP2 is completely degraded in ∼65% of cells with nuclear-localized ndCKAP2 within one cell cycle (24 hours for HeLa cells), nuclear ndCKAP2 may be visible in high expressing cells for up to several days. Imaging supports this

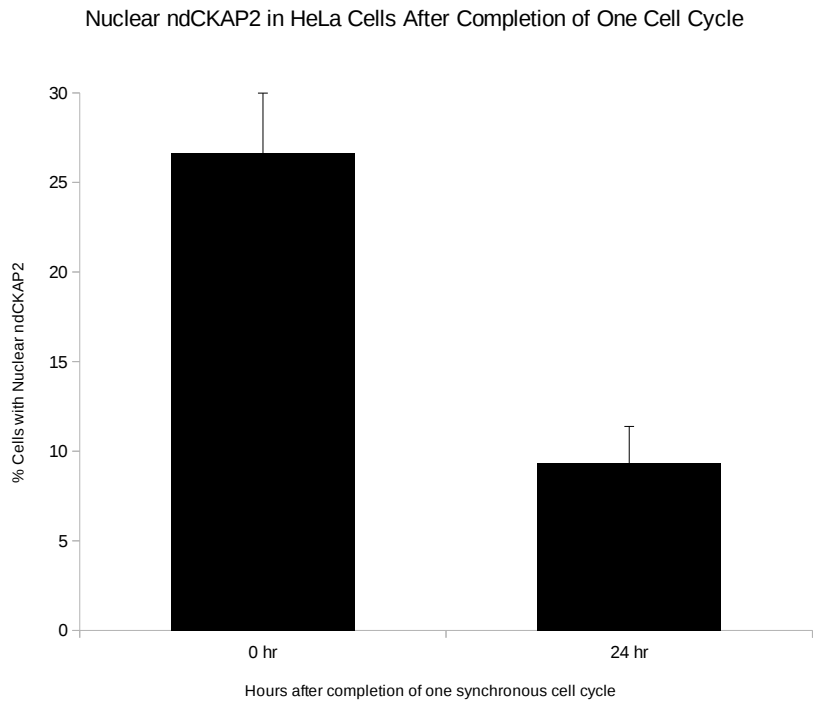

Figure 3.16: Determination of cell population half-life of nuclear-localized GFP-ndCKAP2 in HeLa cells by analysis of proportion of cells with nuclear ndCKAP2. Cells that had completed one synchronous cell cycle were blocked from re-entering cell cycle and analyzed. Data shown is mean ± SD, with $N = 4$ and > 150 cells per sample. The difference in proportion of cells with nuclear ndCKAP2 between the 0hr and 24 hr groups was statistically significant ($p < 0.05$), as determined by a one-tailed Student's t-test.

claim; cells displaying nuclear ndCKAP2 were observed 48 hours after completion of synchronous cell cycle (Figure 3.15). Thus, half-life calculations demonstrate the integrative capacity of GFP-ndCKAP2.

Chapter 4

Discussion

The aim of this investigation was to establish ndCKAP2 as a cell division probe that could serve as a tool to assess cardiomyocyte proliferation. In particular, to meet the challenges of assessing cardiomyocyte proliferation [14, 17, 32], it was necessary to demonstrate that the ndCKAP2 molecular probe would be easily visualized, unambiguous in identification of proliferation, and integrative in nature. To this end, an eGFP-ndCKAP2 fusion protein was generated by subcloning into a lentiviral vector; moreover, this vector was used to produce lentivirus carrying the molecular probe. The expression of the probe, both by liposome-mediated transfection and viral transduction, was verified in a variety of cell types, including NRCMs. The probe was then assessed for its ability to mark mitotic events by performing cell cycle analysis in a proliferative cell type. Finally, the half-life was calculated to demonstrate the integrative nature of the probe.

Figures 3.6 and 3.7 shows the expression of GFP-ndCKAP2 in both immortalized cells (HeLa, HEK293, and NIH3T3) as well as in primary cells (NRCMs and CSCs).

Examples of both cytoplasmic and nuclear figures are highlighted as well. The localization of ndCKAP2 matches predictions based on prior literature [51, 52, 53]. As can be seen in Figure 3.5, cytoplasmic ndCKAP2 shows a distinct microtubule association, verified by staining cells with α-tubulin. Similarly, nuclear localization of ndCKAP2 matches DAPI staining. The distinction between cytoplasmic and nuclear ndCKAP2 is readily seen under fluorescent microscopy, thus satisfying the criteria for the GFP-ndCKAP2 molecular probe to be easily visualized. Expression of GFP-ndCKAP2 was successful with both transfection and transduction, satisfying the aim to generate a fluorescent cell division probe.

Nuclear ndCKAP2 was seen in all proliferative cell types within one day of culture, but absent in NRCMs even after one week of culture. Mammalian cardiomyocytes are known to undergo DNA synthesis in culture [55]; indeed, staining for BrdU after one week in culture demonstrated evidence of DNA synthesis (data not shown). Thus, the absence of nuclear ndCKAP2 in NRCMs supports the prediction that change in localization of ndCKAP2 is a result of mitosis and not merely DNA synthesis. To further demonstrate that ndCKAP2 unambiguously marks mitotic events, the presence of nuclear ndCKAP2 in cells synchronously proceeding through cell cycle was analyzed. HeLa cells transfected with GFP-ndCKAP2 were synchronized at the G_1/S border by a double thymidine block; after re-release into cell cycle, cells were serially harvested and analyzed for localization of GFP-ndCKAP2. Figure 3.9 shows that cells displaying nuclear ndCKAP2 are only observed after 8 hours post-release from double thymidine block; these results correspond well to progression through cell cycle demonstrated by both flow cytometry of PI-stained cells and PHH3 staining. More-

over, cells with nuclear ndCKAP2 almost always appeared in pairs (as in Figure 3.10) and closely associated; these data support the hypothesis that nuclear localization of ndCKAP2 is a result of mitosis. In addition, thymidine-nocodazole experiments show that localization occurs after *completion* of mitosis, not merely its onset. Nocodazole arrests cells in prometaphase; however, GFP-ndCKAP2$^+$ cells in prometaphase did not display nuclear localization of the probe (Figure 3.12). These considerations are particularly relevant to a probe that is proposed for use with cardiac cells. Cardiomyocytes have been documented to undergo a number of abortive variants of cell cycle [18], including DNA synthesis without division or onset of mitosis without cytokinesis (endomitosis). GFP-ndCKAP2 unambiguously differentiates between these various cell cycle phenomena, making it well-suited for studying proliferation in the heart.

If proliferation occurs in the heart, whether under physiological or injury conditions, the rate of proliferation is likely to be very low. Thus, one of the main strengths of GFP-ndCKAP2 as a probe for assessing cardiomyocyte proliferation is its integrative nature, i.e. its ability to track mitotic events that *have already happened* as opposed to merely events that are in the process of happening at time of analysis. ndCKAP2 contains a mutation in a key region of the protein known as the KEN box, which plays a role in binding to the anaphase-promoting complex (and promoting breakdown of CKAP2) [52]; however, it was predicted that nuclear ndCKAP2 would eventually be subject to breakdown pathways within the cell. Here, two methods were utilized to determine the half-life of GFP-ndCKAP2 once translocated to the nucleus following completion of cell division. On the basis of the events of nuclear ndCKAP2 that "disappear" following completion of round of mitosis, the half-life

of GFP-ndCKAP2 is approximately 16 hours (Figure 3.14). By way of comparison, PHH3 expression begins to decline shortly after completion of anaphase. Another recent probe used for cardiomyocyte proliferation, GFP-anillin, shows expression for only up to 86 minutes post-mitosis [33]. However, while GFP-ndCKAP2 is broken down in a large number of cells within completion of a second cell cycle, high expressors of GFP-ndCKAP2 may continue to express nuclear ndCKAP2 for up to about 76 hours; indeed, cells displaying nuclear ndCKAP2 were seen 48 hours after thymidine arrest following completion of one round of cell cycle. In another experiment (not shown here), a GFP-ndCKAP2 stably-transduced HEK293 cell line was generated via blasticidin selection. While initially all of the cells demonstrated cytoplasmic ndCKAP2, within 2 - 3 weeks of culture cells with nuclear ndCKAP2 accumulated and formed the majority of the line. Further analysis may be useful in understanding the breakdown of nuclear ndCKAP2; in particular, the mechanism of breakdown of nuclear ndCKAP2 may be of interest. It is possible that ndCKAP2 presents some nuclear export sequence that eliminates the nuclear protein despite mutation in the motif that mediates breakdown by ubiqutin-proteosome pathways. Future experimentation may seek to uncover and manipulate such sites to improve the half-life of nuclear ndCKAP2. Taken together, these results support the integrative nature of ndCKAP2.

The strong expression of GFP-ndCKAP2 in NRCMs after viral transduction suggests that lentivirus is a particularly suitable method for introducing the molecular ndCKAP2 probe to cardiomyocytes for *in vitro* (and potentially *in vivo*) analysis. In particular, lentiviral transduction of cardiomyocytes with GFP-ndCKAP2 could be

used to assess and quantify the effects of various proposed growth factor cocktails on cardiomyocyte proliferation *in vitro*. Currently, a number of studies have suggested induction of cardiomyocyte cell cycle and mitosis *in vitro* via therapies such as FGF1, NRG1, and periostin [38, 39, 40, 41, 42]. There is currently no standard for determining proliferation of cardiomyocytes in these systems, and the authors alternatively use cell counting [40] and/or immunohistochemistry for a variety of markers such as PHH3 or Aurora B Kinase [39, 40, 42]. Each of these methods requires complex processing of the tissues. Moreover, in some experiments, the doubling time of cardiomyocytes with treatment is as long as 4 - 5 days [41]; by way of comparison, HeLa cells have a doubling time of 24 hours. Compared to these methods, use of GFP-ndCKAP2 as a probe in cardiomyocytes *in vitro* requires little processing; cells need to be transduced and then imaged under fluorescent microscope. The strong expression of GFP-ndCKAP2 in NRCMs, as seen in Figure 3.7c, obviates the need for fixation and staining as well. Thus, GFP-ndCKAP2 could prove to be a powerful standard for ascertaining the capacity of various proposed therapeutics to induce cardiomyocyte proliferation. Indeed, a future goal of this investigation is to test the above growth factor therapies on NRCMs transduced with GFP-ndCKAP2. Early results failed to replicate the claims, for example, of Engel et al. that FGF1/p38 MAPKi could be used to stimulate cardiomyocyte proliferation (data not shown here), though the possibility of experimental error must be ruled out before any definitive conclusions are made about the therapeutic approach. Further work with GFP-ndCKAP2 could be used to support the translation of proposed growth factor cocktails into clinical trials, and may aid in the identification of new therapeutic avenues.

Though engineered to meet the demands of cardiac systems, GFP-ndCKAP2 is not limited in use to the study of cardiomyocyte proliferation. Figures 3.6 and 3.7 verify the wide range of cell types with which GFP-ndCKAP2 can be used, including commonly used transformed cell lines such as HeLa, HEK293, and NIH3T3. Of particular interest is that GFP-ndCKAP2 can be introduced via lentiviral transduction to stem cells (here, human c-Kit$^+$ cardiac stem cells) with high level of expression. Characterizing stem cells has been a major challenge in the field of regenerative medicine and, indeed, different stem cell lines have been shown to have greatly differing phenotype [56]. In the cardiac stem cell field, c-Kit$^+$ progenitors derived from different patients have different level of expression of c-Kit as well different proliferation rates. Some cell lines in particular proliferate at an extremely low rate. The integrative nature of GFP-ndCKAP2 makes it an ideal probe to assess proliferation rates and doubling time in these slowly dividing cell lines. In this sense, GFP-ndCKAP2 could be used to characterize cell cycle behaviour for stem cell populations.

One particular weakness to the use of ndCKAP2 as a proliferation probe is that ndCKAP2 overexpression may result in spindle defects and failure of cytokinesis [52]. Some researchers have documented the formation of monopolar mitotic spindles or other microtubule aberrations in cells transfected with ndCKAP2, preventing progression through mitosis. Here, these results were not replicated; indeed, cell cycle profiles of asynchronous and synchronous HeLa cells transfected with GFP-ndCKAP2 matched those of cells transfected with a GFP control (not shown here). Moreover, in synchronous cell cycle experiments, very few cells with unusual microtubule patterns were observed before or after completion of mitosis. Similarly, observations of

the GFP-ndCKAP2 stably-transduced HEK293 cell line did not present abnormal spindle defects similar to those reported in the literature, and GFP-ndCKAP2$^+$ cells continued to proliferate for several weeks. Nevertheless, the possibility that expression of ndCKAP2 may affect completion of mitosis must be considered more thoroughly to establish ndCKAP2 as a useful proliferation probe. One possible approach would be to determine whether differing expression levels (as controlled by amount of DNA/virus used to transfect/transduce cells) result in spindle defects. Careful calibration may largely eliminate these concerns.

Thus, here a new approach to assessing cardiomyocyte proliferation has been developed. Based on the design requirements of the cardiomyocyte system, a GFP-ndCKAP2 molecular probe has been developed; moreover, this study establishes the probe as being easily visualizable, unambiguous in its marking of mitotic events, and integrative in nature. It is hoped that future applications of this molecular probe may allow for the discovery of new insights into cardiac proliferation and renewal, and may be used to guide the development of therapies for patients suffering from cardiac damage and cardiomyocyte insufficiency.

Bibliography

[1] A. S. Go et al. Heart disease and stroke statistics - 2013 update: A report from the american heart association. *Circulation*, **127**:e6 – e245, 2012.

[2] M.A. Laflamme & C.E. Murry. Heart regeneration. *Nature*, **473**:326 – 335, 2011.

[3] C.E. Murry et al. Regeneration gaps: Observations on stem cells and cardiac repair. *Journal of the American College of Cardiology*, **47**:1777 – 1785, 2006.

[4] R.S. Whelan et al. Cell death in the pathogenesis of heart disease: Mechanisms and significance. *Annual Review of Physiology*, **72**:19 – 44, 2009.

[5] G. Olivetti et al. Cardiomyopathy of the aging human heart: Myocyte loss and reactive cellular hypertrophy. *Circulation Research*, **68**:1560 – 1568, 1991.

[6] Y. Sun. Myocardial repair/remodelling following infarction: roles of local factors. *Cardiovascular Research*, **81**:482 – 490, 2009.

[7] C.L. Mummery. Solace for the broken-hearted? *Nature*, **433**:585 – 587, 2005.

[8] Z.W. Tao & L.G. Li. Cell therapy in congestive heart failure. *Journal of Zhejiang University SCIENCE B*, **8**:647 – 660, 2007.

[9] O. Bergmann et al. Evidence for cardiomyocyte renewal in humans. *Science*, **324**:98 – 102, 2009.

[10] M. Mollova et al. Cardiomyocyte proliferation contributes to heart growth in young humans. *Proceeds of the National Academy of Sciences*, **110**:1446 – 1451, 2013.

[11] J. Kajstura et al. Myocyte turnover in the aging human heart. *Circulation Research*, **107**:1374 – 1386, 2010.

[12] J. Kajstura et al. Cardiomyogenesis in the aging and failing human heart. *Circulation*, **126**:1869 – 1881, 2012.

[13] J. Kajstura et al. Cardiomyogenesis in the adult human heart. *Circulation Research*, **107**:305 – 315, 2010.

[14] K. Malliaras & J. Terrovitis. Cardiomyocyte proliferation vs progenitor cells in myocardial regeneration: The debate continues. *Global Cardiology Science and Practice*, **3**:37 – 51, 2013.

[15] A.P. Beltrami et al. Evidence that human cardiac myocytes divide after myocardial infarction. *The New England Journal of Medicine*, **344**:1750 – 1757, 2001.

[16] K. Malliaras et al. Cardiomyocyte proliferation and progenitor cell recruitment underlie therapeutic regeneration after myocardial infarction in the adult mouse heart. *EMBO Molecular Medicine*, **5**:191 – 209, 2013.

[17] F.B. Engel. Cardiomyocyte proliferation: A platform for mammalian cardiac repair. *Cell Cycle*, **4**:1360 – 1363, 2005.

[18] K.B.S. Pasumarthi & L.J. Field. Cardiomyocyte cell cycle regulation. *Circulation Research*, **90**:1044 – 1054, 2002.

[19] P. Anversa et al. Myocyte mitotic division in the aging mammalian rat heart. *Circulation Research*, **69**:1159 – 1164, 1991.

[20] P. Anversa & J. Kajstura. Ventricular myocytes are not terminally differentiated in the adult mammalian heart. *Circulation Research*, **83**:1 – 14, 1998.

[21] P.C.H. Hsieh et al. Evidence from a genetic fate-mapping study that stem cells refresh adult mammalian cardiomyocytes after injury. *Nature Medicine*, **13**:970 – 974, 2007.

[22] E.R. Porrello et al. Transient regenerative potential of the neonatal mouse heart. *Science*, **331**:1078 – 1080, 2011.

[23] M. Mercola et al. Cardiac muscle regeneration: lessons from development. *Genes and Development*, **25**:299 – 309, 2011.

[24] A.P. Beltrami et al. Adult cardiac stem cells are multipotent and support myocardial regeneration. *Cell*, **114**:763 – 776, 2003.

[25] H. Oh et al. Cardiac progenitor cells from adult myocardium: Homing, differentiation, and fusion after infarction. *Proceedings of the National Academy of Sciences*, **100**:12313 – 12318, 2003.

[26] E. Messina et al. Isolation and expansion of adult cardiac stem cells from human and murine heart. *Circulation Research*, **95**:911 – 921, 2004.

[27] J.O. Oberpriller & J.C. Oberpriller. Response of the adult newt ventricle to injury. *Journal of Experimental Zoology*, **187**:249 – 260, 1974.

[28] A.W. Neff et al. Heart development and regeneration in urodeles. *International Journal of Developmental Biology*, **40**:719 – 725, 1996.

[29] K.D. Poss et al. Heart regeneration in zebrafish. *Science*, **298**:2188 – 2190, 2002.

[30] K. Kikuchi et al. Primary contribution to zebrafish heart regeneration by *gata4*$^+$ cardiomyocytes. *Nature*, **464**:601 – 605, 2010.

[31] M. Xin et al. Mending broken hearts: cardiac development as a basis for adult heart regeneration and repair. *Nature Reviews: Molecular Cell Biology*, **14**:529 – 541, 2013.

[32] M.J. van Amerongen & F.B. Engel. Features of cardiomyocyte proliferation and its potential for cardiac regeneration. *Journal of Cell and Molecular Medicine*, **12**:2233 – 2244, 2008.

[33] M. Hesse et al. Direct visualization of cell division using high-resolution imaging of m-phase of the cell cycle. *Nature Communications*, **3**, 2012.

[34] E.B. Katz et al. Cardiomyocyte proliferation in mice expressing α-cardiac myosin heavy chain-sv40 t-antigen transgenes. *American Journal of Physiology*, **262**:H1876 – 1876, 1992.

[35] X. Yuan & T. Braun. An unexpected switch: Regulation of cardiomyocyte proliferation by the homeobox gene *Meis1*. *Circulation Research*, **113**:245 – 248, 2013.

[36] N. Liu et al. microrna-133a regulates cardiomyocyte proliferation and suppresses smooth muscle gene expression in the heart. *Genes and Development*, **22**:3242 – 3254, 2008.

[37] H.J. Evans-Anderson et al. Regulation of cardiomyocyte proliferation and myocardial growth during development by foxo transcription factors. *Circulation Research*, **102**:686 – 694, 2008.

[38] T. Braun & S. Dimmeler. Breaking the silence: Stimulating proliferation of adult cardiomyocytes. *Developmental Cell*, **17**:151 – 152, 2009.

[39] K. Bersell et al. Neuregulin1/erbb4 signaling induces cardiomyocyte proliferation and repair of heart injury. *Cell*, **138**:257– 270, 2009.

[40] F.B. Engel et al. p38 map kinase inhibition enables proliferation of adult mammalian cardiomyocytes. *Genes and Development*, **19**:1175 – 1887, 2005.

[41] F.B. Engel et al. Fgf1/p38 map kinase inhibitor therapy induces cardiomyocyte mitosis, reduces scarring, and rescues function after myocardial infarction. *Proceedings of the National Academy of Sciences*, **103**:15546 – 15551, 2006.

[42] Berhand Kühn et al. Periostin induces proliferation of differentiated cardiomyocytes and promotes cardiac repair. *Nature Medicine*, **13**:962 – 969, 2007.

[43] K.L. Ang et al. Limitations of conventional approaches to identify myocyte nuclei in histologic sections of the heart. *American Journal of Physiology Cell Physiology*, **298**:C1603 – C1609, 2010.

[44] M.H. Soonpaa & L.J. Field. Survey of studies examining mammalian cardiomyocyte dna synthesis. *Circulation Research*, **83**:15 – 26, 1998.

[45] N. Kee et al. The utility of ki-67 and brdu as proliferative markers of adult neurogenesis. *Journal of Neuroscience Methods*, **115**:97 – 105, 2002.

[46] Anonymous Abreview, Abcam. Anti-brdu antibody (biotin) (ab2284). http://www.abcam.com/brdu-antibody-biotin-ab2284.html/reviews/6869

[47] A.A. Van Hooser et al. The perichromosomal layer. *Chromosoma*, **114**:377 – 388, 2005.

[48] M.J. Hendzel et al. Mitosis-specific phosphorylation of histone h3 initiates primarily within pericentromeric heterochromatin during g2 and spreads in an ordered fashion coincident with mitotic chromosome condensation. *Chromosoma*, **106**:348 – 360, 1997.

[49] L. Lewellyn et al. The chromosomal passenger complex and centralspindlin independently contribute to contractile ring assembly. *Journal of Cell Biology*, **193**:155 – 169, 2011.

[50] J. Low et al. High-content imaging characterization of cell cycle therapeutics through *in vitro* and *in vivo* subpopulation analysis. *Molecular Cancer Therapeutics*, **7**:2455 – 2463, 2008.

[51] K.U. Hong et al. Tmap/ckap2 is essential for proper chromosome segregation. *Cell Cycle*, **8**:314 – 324, 2009.

[52] K.U. Hong et al. Functional importance of the anaphase-promoting complexcdh1-mediated degradation of tmap/ckap2 in regulation of spindle function and cytokinesis. *Molecular and Cellular Biology*, **27**:3667 – 3681, 2007.

[53] K.U. Hong et al. Cdk1-cyclin b1-mediated phosphorylation of tumor-associated microtubule-associated protein/cytoskeleton-associated protein 2 in mitosis. *Journal of Biological Chemistry*, **284**:16501 – 16512, 2009.

[54] H.S. Kim et al. Condensed chromatin staining of ckap2 as surrogate marker for mitotic figures. *Journal of Cancer Research and Clinical Oncology*, **138**:95 – 102, 2012.

[55] A.C. Nag et al. Competence of embryonic mammalian heart cells in culture: Dna synthesis, mitosis and differentiation. *Cytobios*, **30**:189 – 208, 1981.

[56] Mari Pekkanen-Mattila et al. Substantial variation in the cardiac differentiation of human embryonic stem cell lines derived and propagated under the same conditions a comparison of multiple cell lines. *Annals of Medicine*, **41**:360 – 370, 2009.